

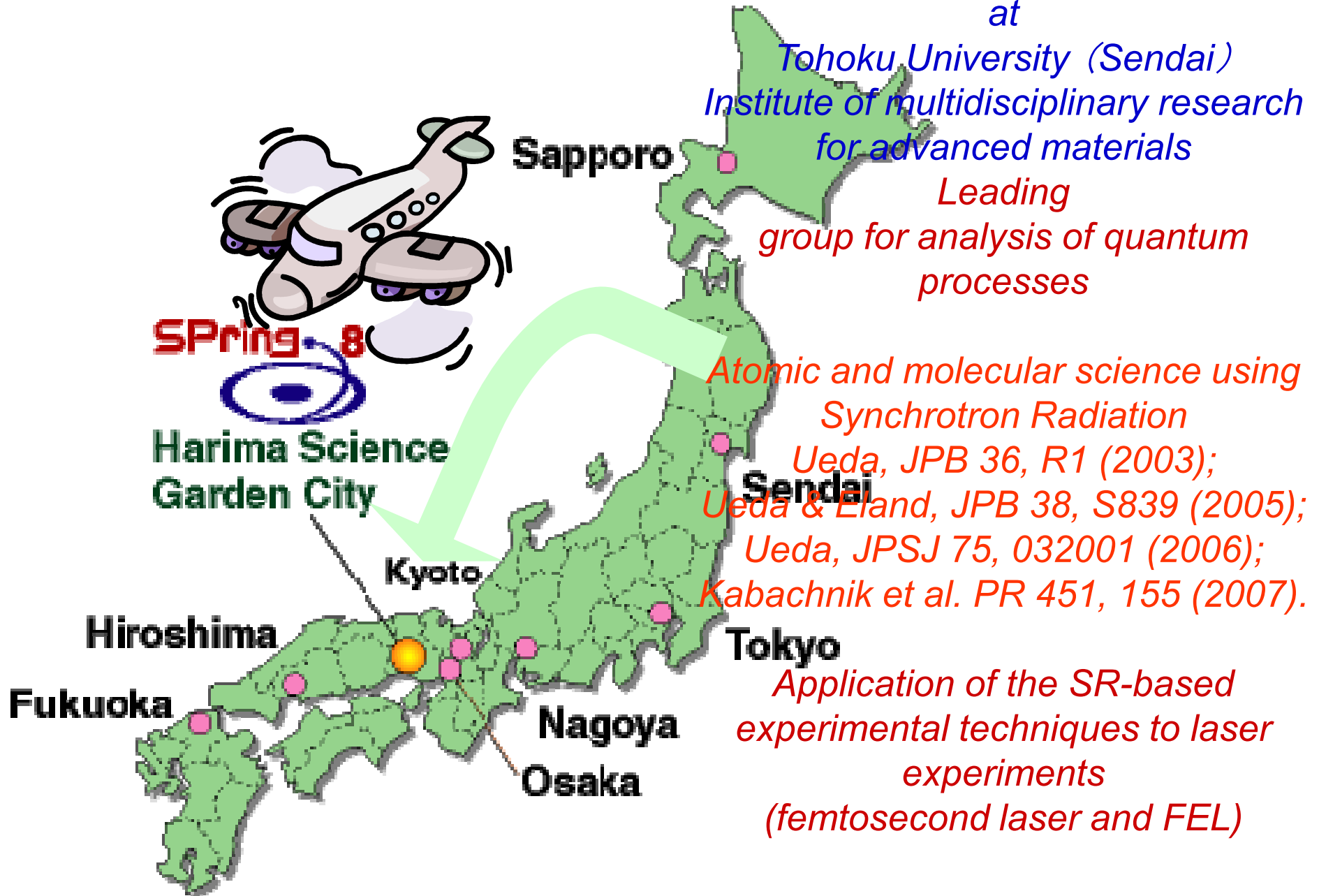
Cheiron School, SPring-8, Japan
October 2, 2008

Studies on atoms and molecules using synchrotron radiation

Kiyoshi Ueda

*Institute of multidisciplinary research for advanced materials
Tohoku University, Sendai 980-8577, Japan*

Introduction of myself



Outline

1. *Introduction to quantum world*
2. *Atomic resonant photoemission spectroscopy*
 - *Introduction to the quantum interference*
3. *Vibrationally-resolved core-level photoelectron spectroscopy*
 - *Franck-Condon analysis and shape resonance effects*
 - *Young's double-slit experiments*
 - *Intermission* -
4. *Multiple-ion momentum imaging*
 - *Snapshots of molecular deformation within a few fs*
5. *Electron-ion momentum imaging*
 - *Molecular frame photoelectron angular distributions*
 - *Interatomic Coulombic decay*

Photoelectric effect

When matter is shined by the light, electron is emitted from the surface.

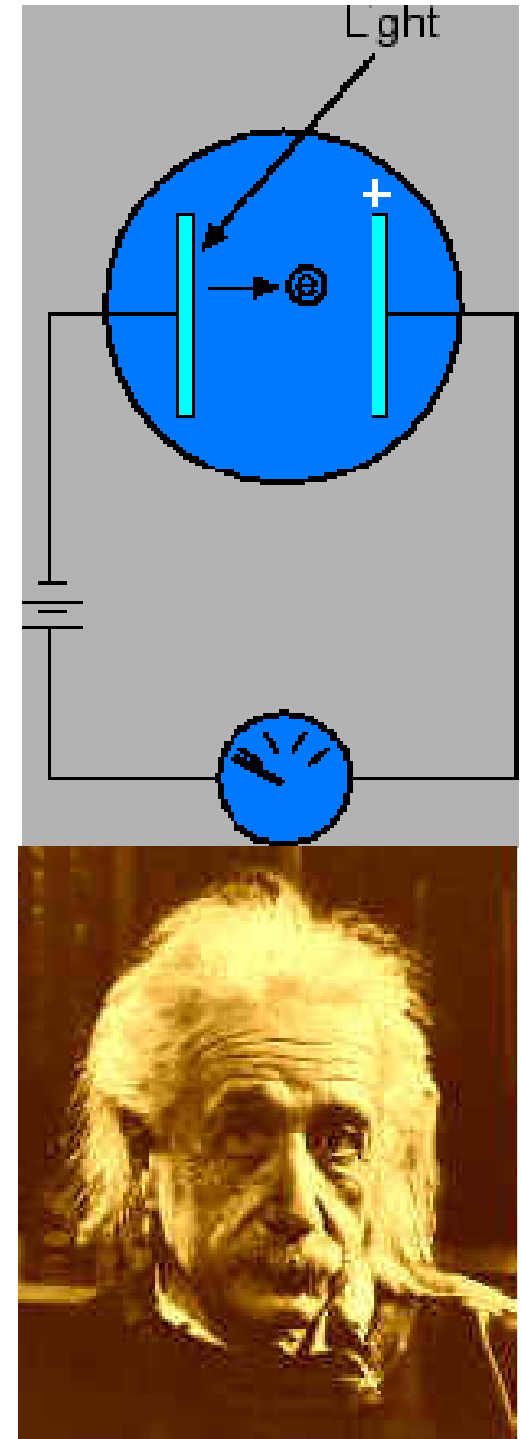
- (i) Frequency of the light needs to be larger than ν_0 .
- (ii) Kinetic energy of the electron is determined by the frequency of the light.
- (iii) Number of electron is proportional to the intensity of the light.

Einstein's explanation

Light at frequency of ν is considered to be a group of particles (photons) and each photon has energy $h\nu$. An electron gets the energy $h\nu$ when it absorbs one photon.

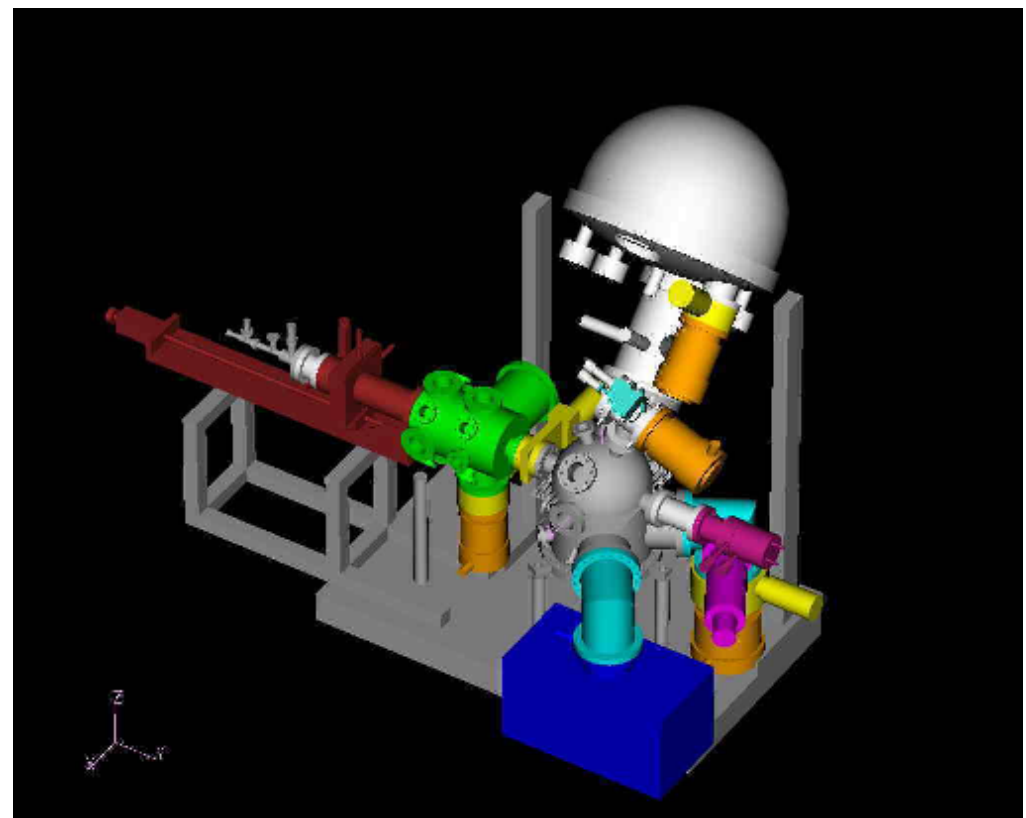
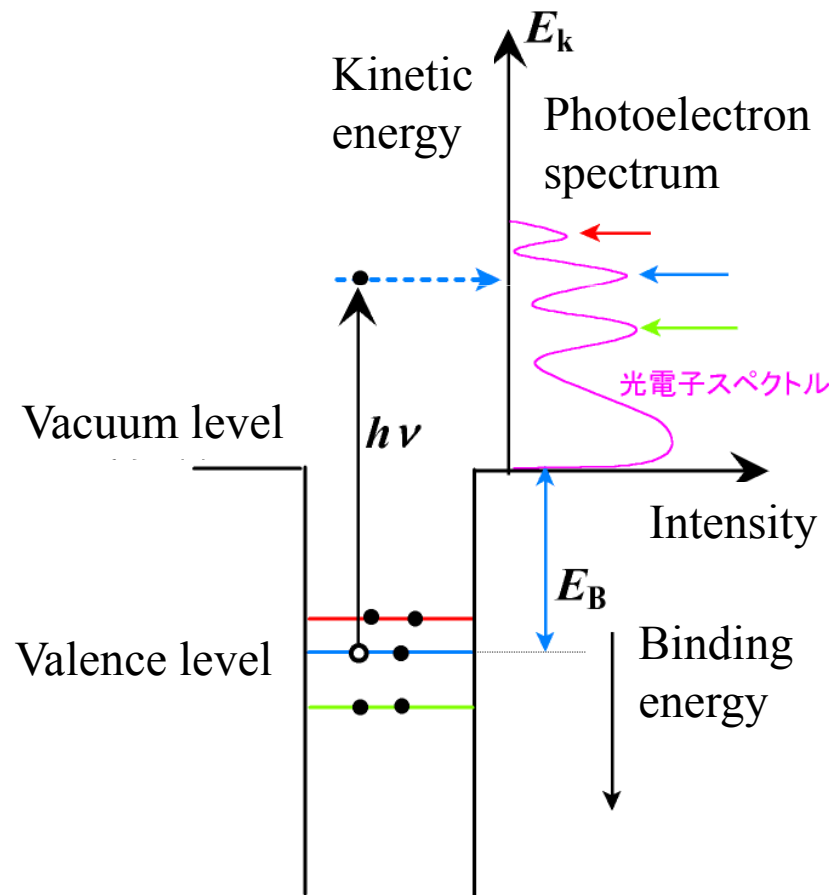
The electron in the matter is bound. For the electron to be emitted from the matter, the electron needs to receive the energy more than the work function W .

Then the kinetic energy KE of the emitted electron can be given as $KE = h\nu - W$.

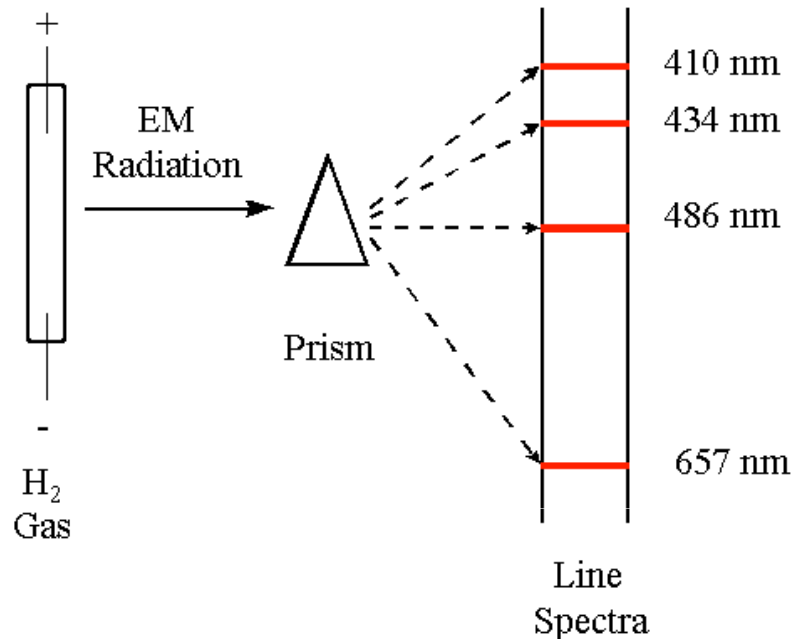


Photoelectron spectroscopy (UPS, XPS)

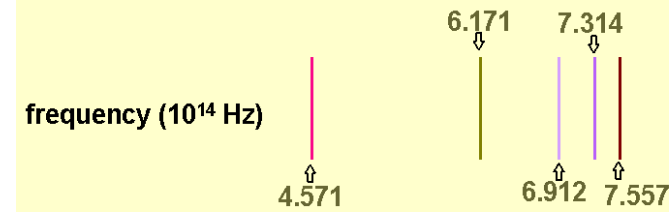
Precision measurements for kinetic energies of photoelectrons emitted via Einstein's photoelectric effects



Balmer and Rydberg formulae



Hydrogen Spectrum: Balmer series



Balmer Formula: $\nu = \nu_0 \left(\frac{1}{n^2} - \frac{1}{m^2} \right)$

$$32.91 \left(\frac{1}{4} - \frac{1}{9} \right) = 4.571$$
$$32.91 \left(\frac{1}{4} - \frac{1}{16} \right) = 6.171$$
$$32.91 \left(\frac{1}{4} - \frac{1}{25} \right) = 6.911$$
$$32.91 \left(\frac{1}{4} - \frac{1}{36} \right) = 7.313$$
$$32.91 \left(\frac{1}{4} - \frac{1}{49} \right) = 7.556$$

IT WORKS!

Balmer found beautiful regularity in the H spectrum!

Rydberg formula : $\frac{\nu}{c} = \frac{1}{\lambda} = R \left(\frac{1}{n^2} - \frac{1}{n'^2} \right)$

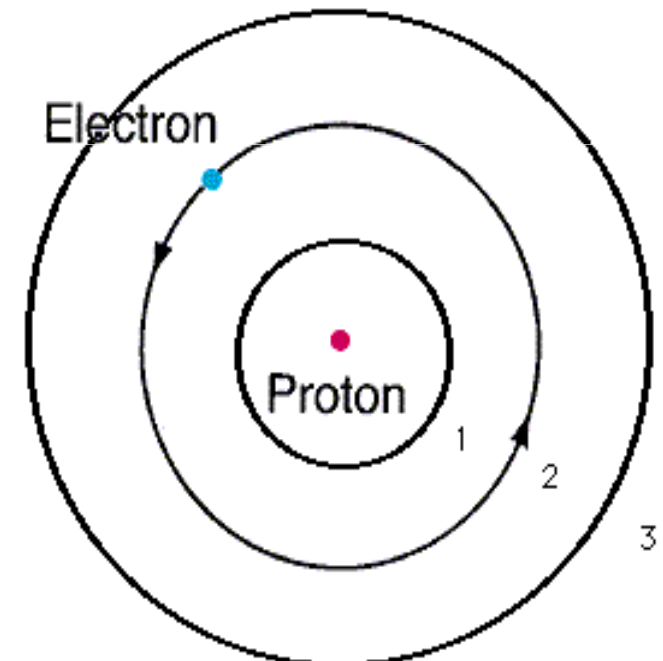
c , speed of light; λ , wavelength; R , Rydberg constant ($R=109737.309 \text{ cm}^{-1}$)

Bohr's atomic model

Electron orbits exist only when the classical orbits satisfy the following condition of quantization:

$$\int_0^{2\pi} p_\varphi \, d\varphi = nh$$

φ , angle of rotation; $p_\varphi = m_e r^2 d\varphi/dt$, angular momentum; r , radius; m_e , electron mass



The electron binding energies are discrete:

$$\bar{E}_n = -hcR/n^2$$

Schrödinger equation of H atom (in atomic units)

$$H\Psi(r) = E\Psi(r)$$

$$H = T + U(r)$$

Hamiltonian

$$T = \frac{p^2}{2} = -\frac{1}{2} \frac{\partial^2}{\partial r^2}$$

kinetic energy

$$p = i \frac{\partial}{\partial r}$$

momentum

$$U(r) = -\frac{1}{r}$$

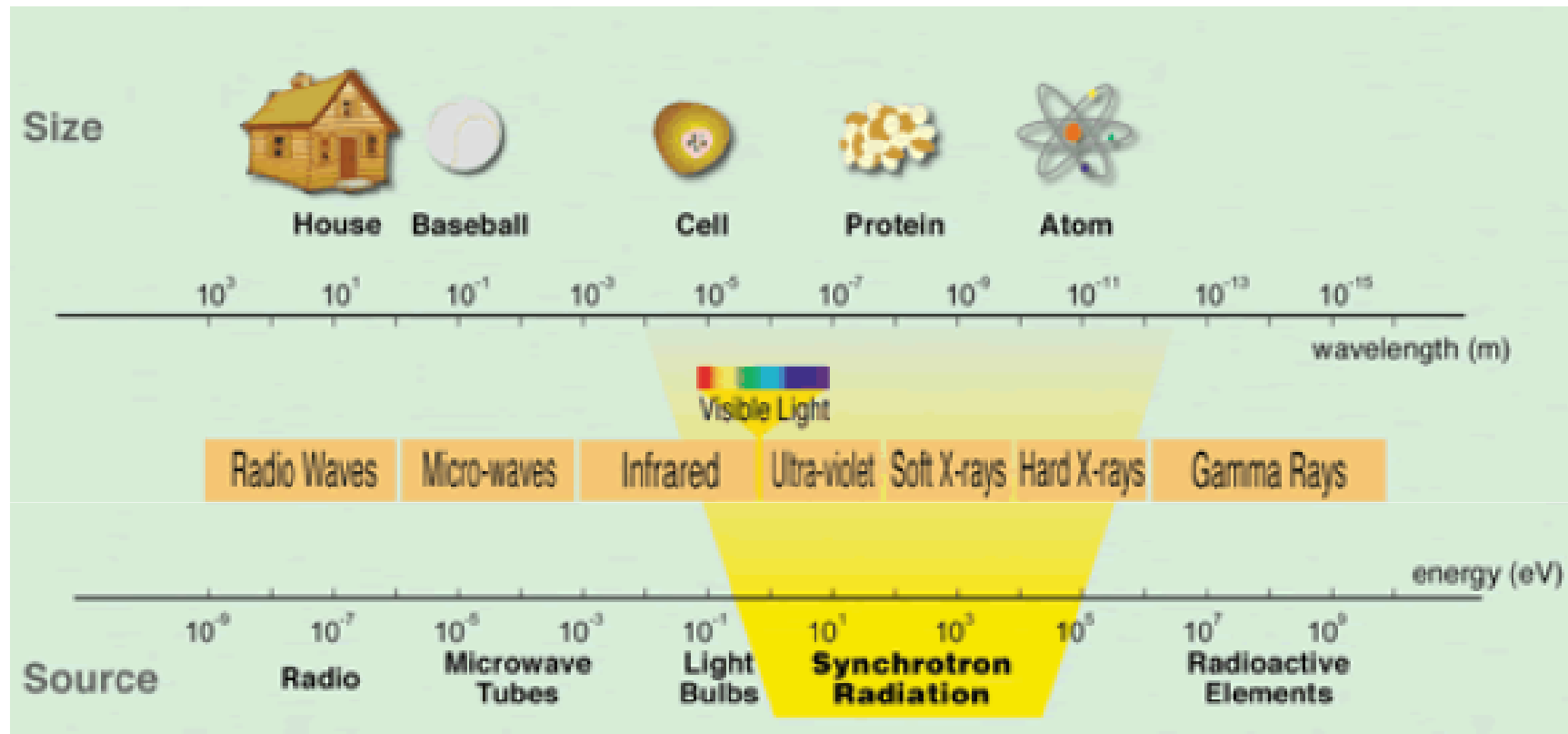
potential energy

$$E_n = -\frac{1}{2n^2}$$

*Ψ : wave function
complex number (with phase!)*

Atomic and molecular science now

Target: single atom or molecule; size: $\sim 1 \text{ \AA}$ ($= 0.1 \text{ nm} = 10^{-10} \text{ m}$)



How to use synchrotron radiation to study atoms and molecules

We use monochromatic synchrotron radiation to excite atoms and molecules and to study their electronic structures as well as electron and nuclear dynamics in the excited states.

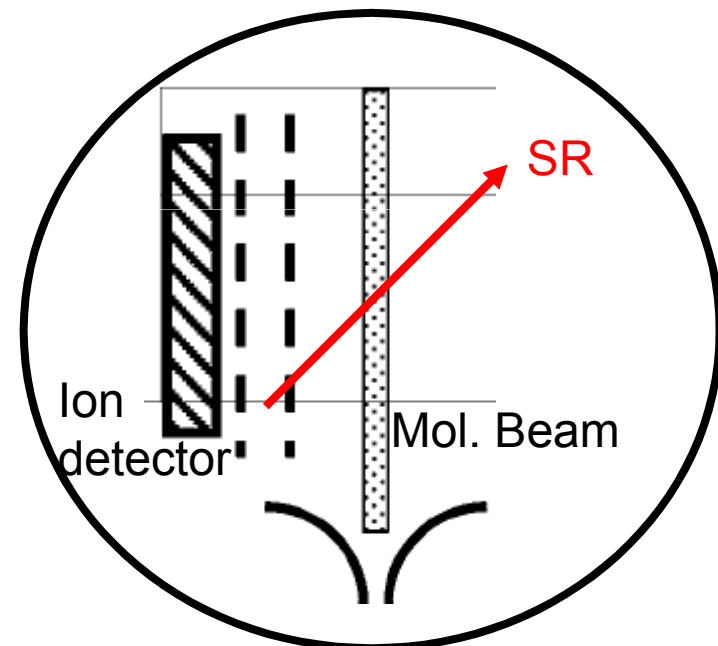
A single photon should be absorbed by a single atom or molecule first!

What photon energies to be used

Electron binding energies (eV) Vacuum ultraviolet light!

Element	K 1s	L ₁ 2s	L ₂ 2p _{1/2}	L ₃ 2p _{3/2}
1 H	13.6			
2 He	24.6*			
3 Li	54.7*			
4 Be	111.5*			
5 B	188*			
6 C	284.2*			
7 N	409.9*	37.3*		
8 O	543.1*	41.6*		
9 F	696.7*			
10 Ne	870.2*	48.5*	21.7*	21.6*

The experiments need to be in the vacuum!



*The easiest experiment:
ion yield spectroscopy*

SPring-8 BL27SU

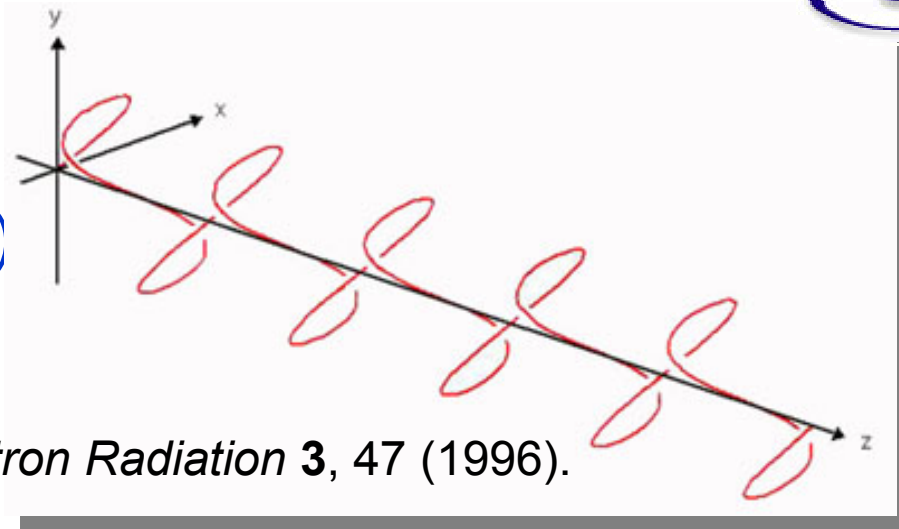


Figure-8 undulator

Linearly polarized light

Horizontal polarization (1st)

Vertical polarization (0.5th)



T. Tanaka and H. Kitamura, *J. Synchrotron Radiation* **3**, 47 (1996).

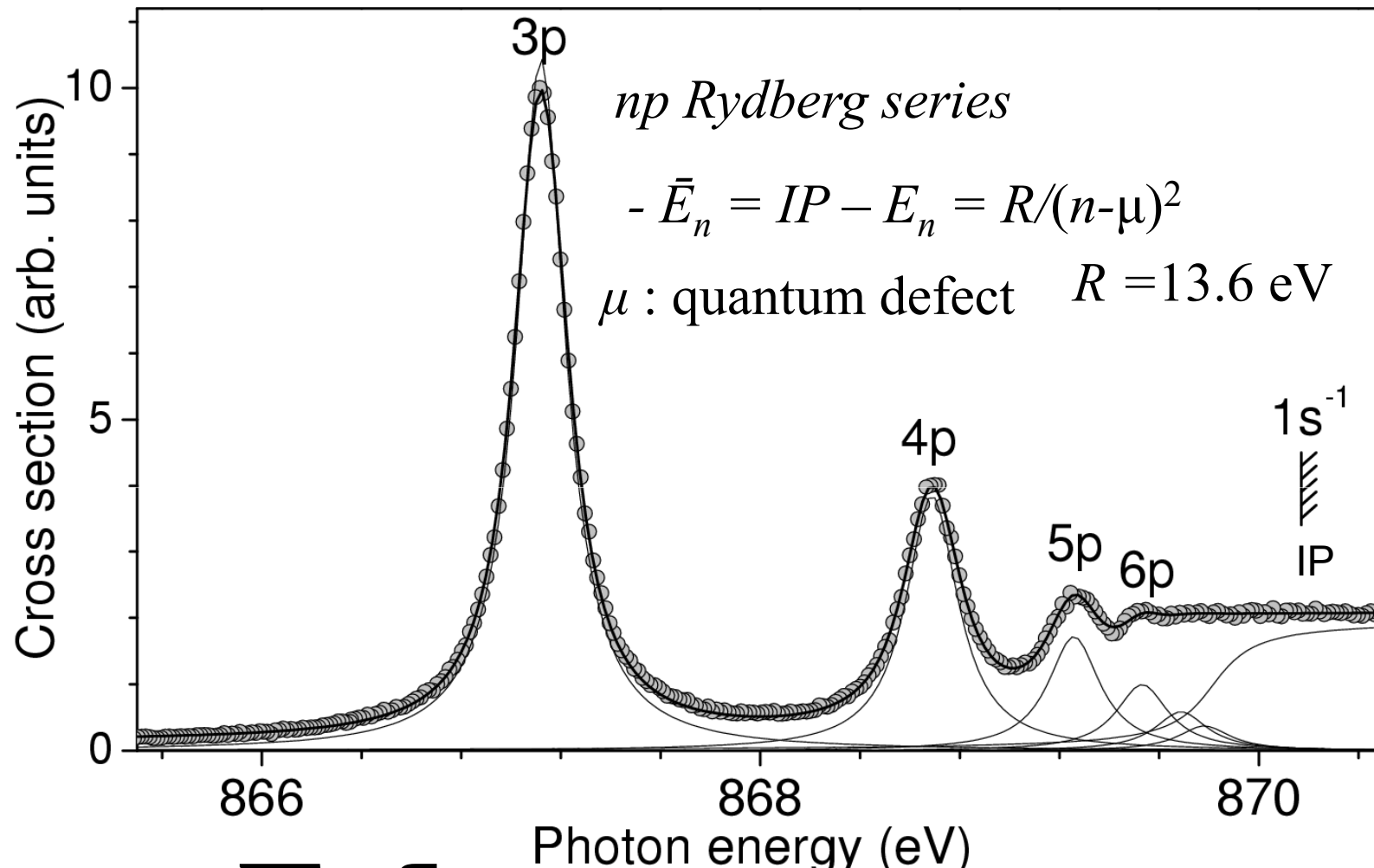
Soft X-ray monochromator

Hettrick type: varied line spacing plane grating

Energy range	0.15 ~ 2.5 keV
Photon Flux	> 10 ¹¹ photon/s
Energy resolution	10000 - 20000

H. Ohashi, Y. Tamenori, E. Ishiguro *et al.* *Nucl. Instr. Methods A* **467**, 533 (2001).

Ne 1s total ion yield spectrum

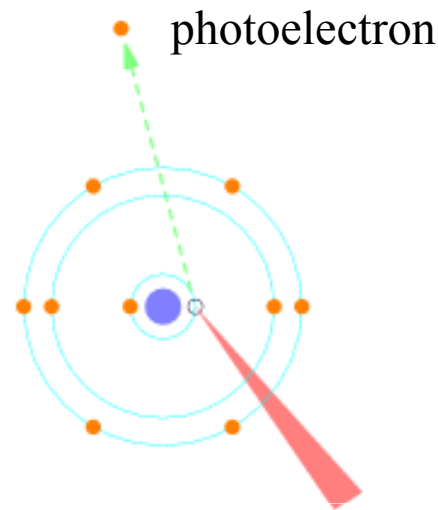


$$\sigma = \sigma_{dir} + \sum_n \frac{\sigma_n}{1+\varepsilon_n^2} + \sigma_{1s} \quad \varepsilon = (h\nu - E_n)/(\Gamma_n/2)$$

$$\sigma_n \propto 1/(n - \mu)^3 \quad \Gamma_n = \text{const!}$$

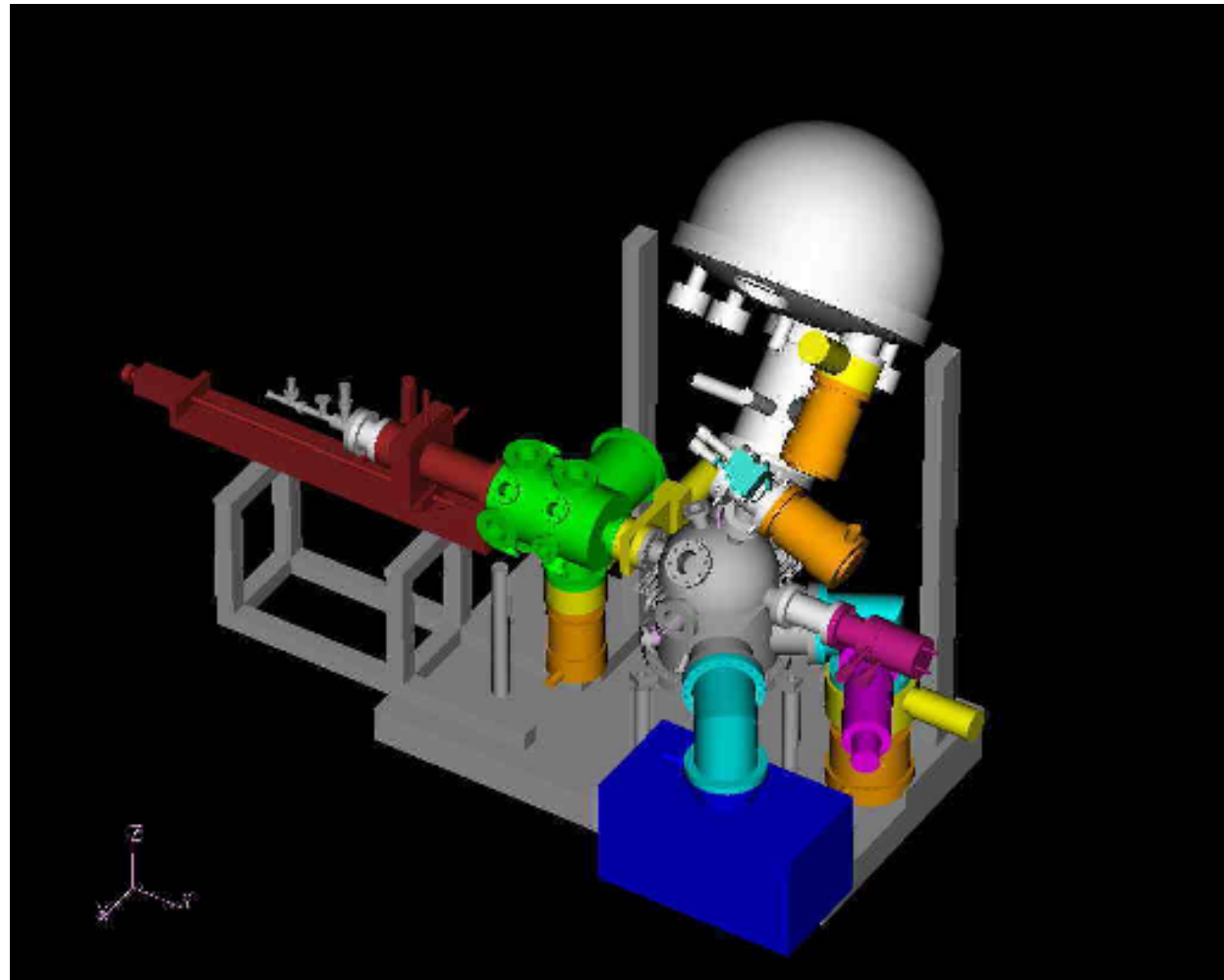
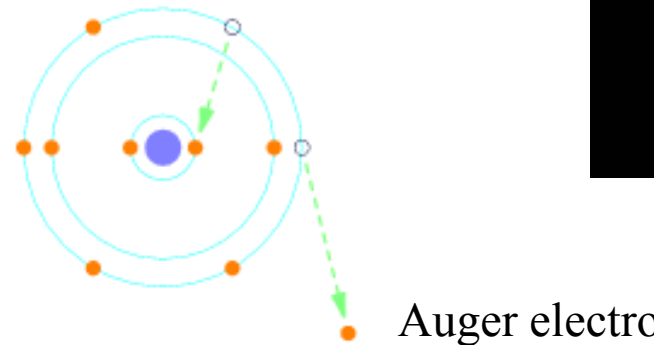
Auger decay and Auger electron spectroscopy

(a) Core ionization



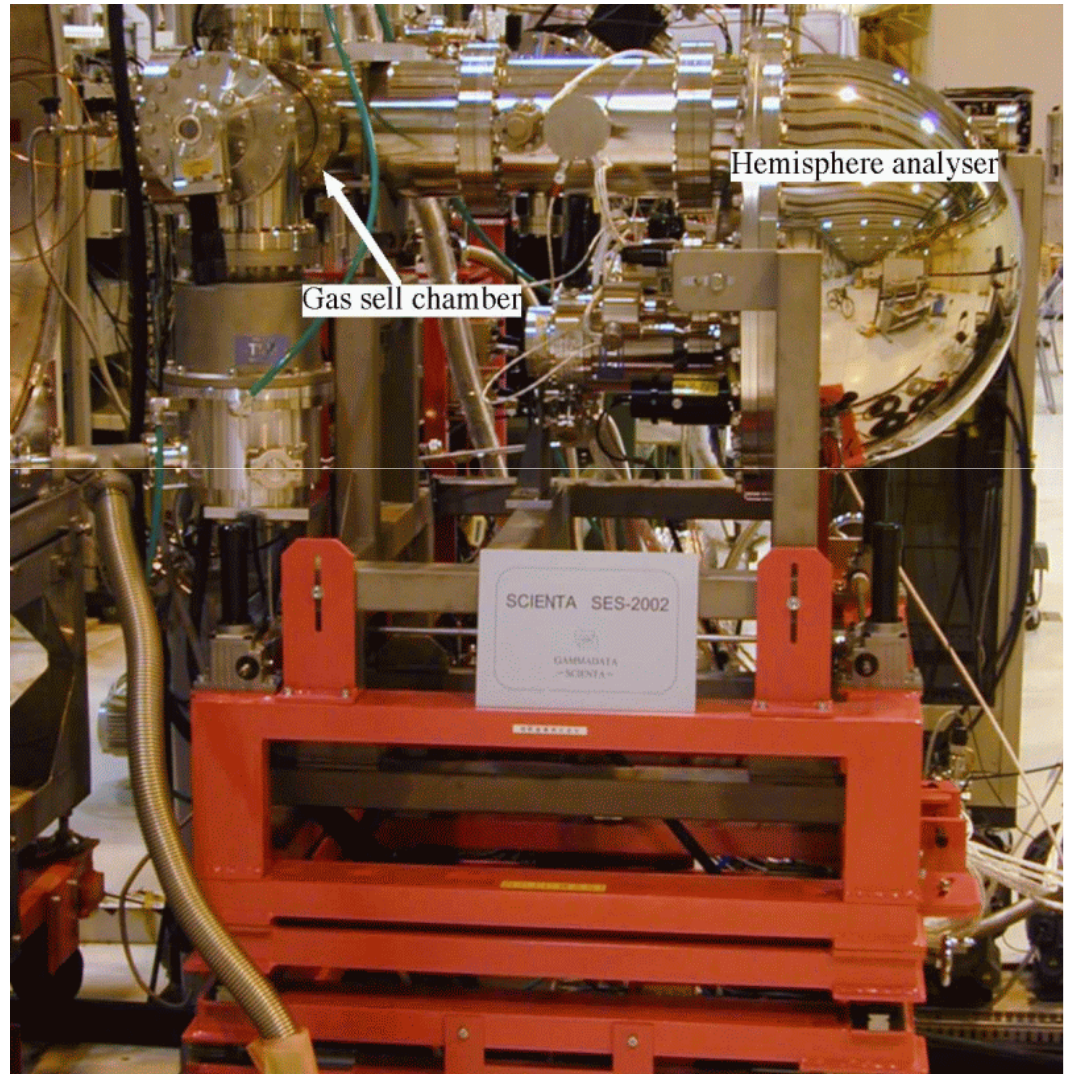
(b) Auger decay:

Core hole lifetime
defines the line width!

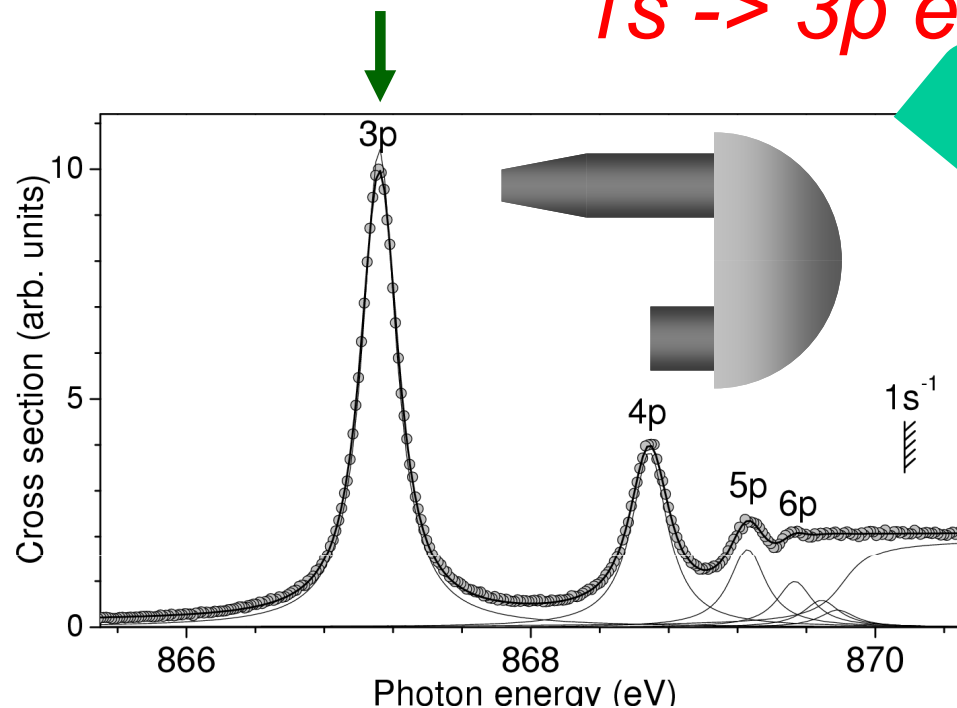


SES2002 analyzer

- Electrostatic hemispherical analyzer
 - Mean radius 200 mm
 - $\Delta E/PE=1/1600$
(66 meV at pass 100 eV)
 - **MCP+CCD camera**
or MCP+Delay line anode
 - **Gas cell system**
or Doppler-free molecular beam source
- Ueda *et al.* *PRL* . **90**, 153005
(2003)
- or effusive beam + momentum resolved ion spectrometer
- Prümper *et al.* *PRA* **71**, 052704,
(2005).



Angle-resolved resonant Auger spectra of Ne at 1s -> 3p excitation

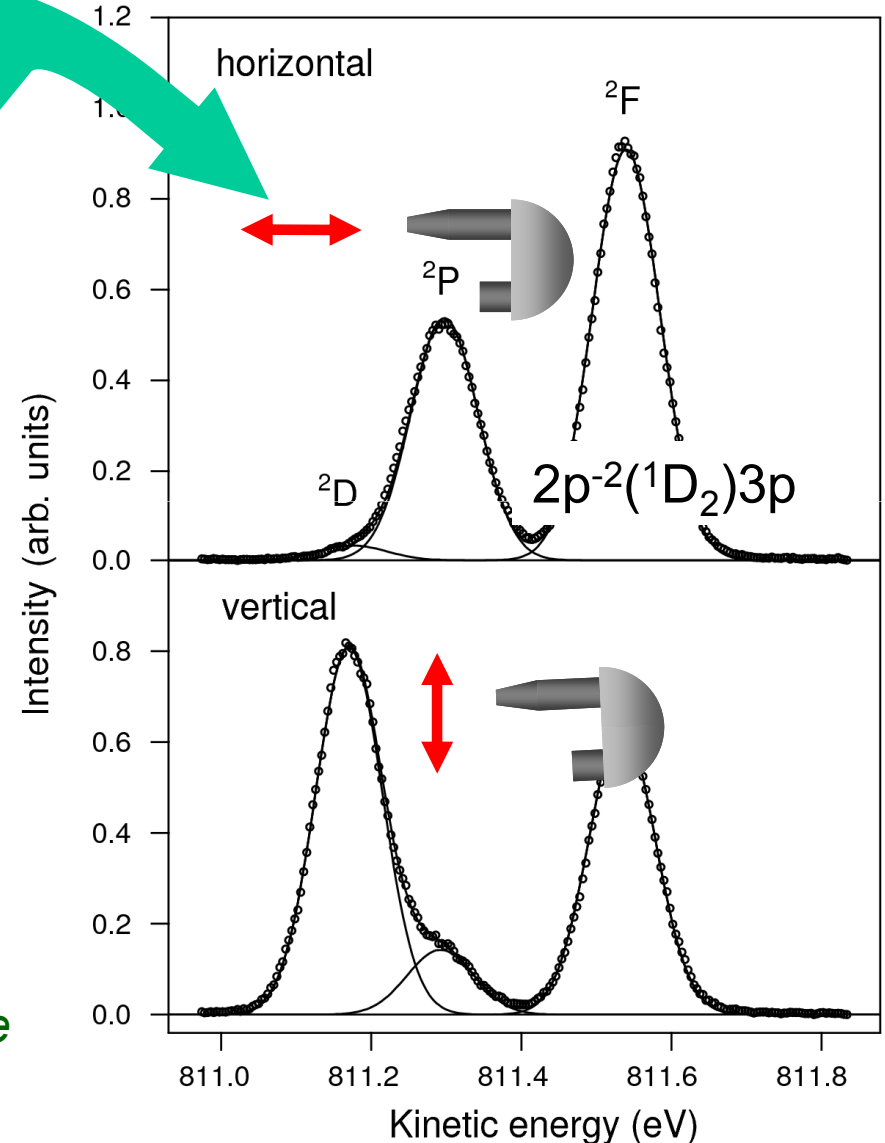


$$\frac{d\sigma}{d\theta} = \frac{\sigma}{4\pi} [1 + \beta P_2(\cos \theta)]$$

$$P_2(\cos \theta) = [3 \cos \theta - 1]/2$$

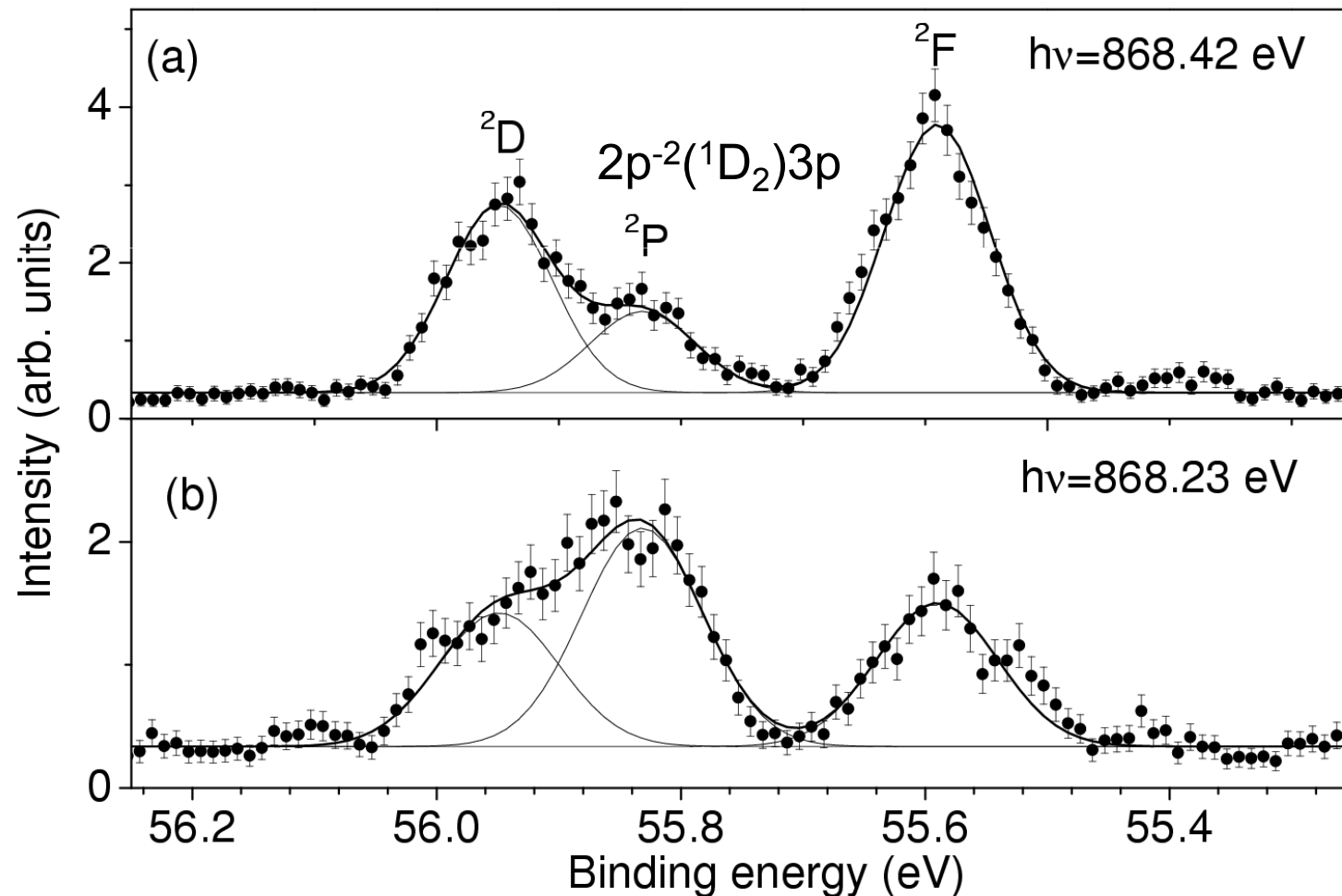
β : asymmetry parameter

Measured angular distributions tell us how the angular momenta are coupled in the atom , allowing us the spectroscopic assignment !



Resonant Auger spectra of Ne “between” $1s \rightarrow 3p$ and $1s \rightarrow 4p$ excitations

$$\frac{d\sigma}{d\theta} = \frac{\sigma}{4\pi}[1 + \beta P_2(\cos \theta)] \quad \sigma \propto I(0) + 2 \times I(90)$$



Interference effects between the two paths

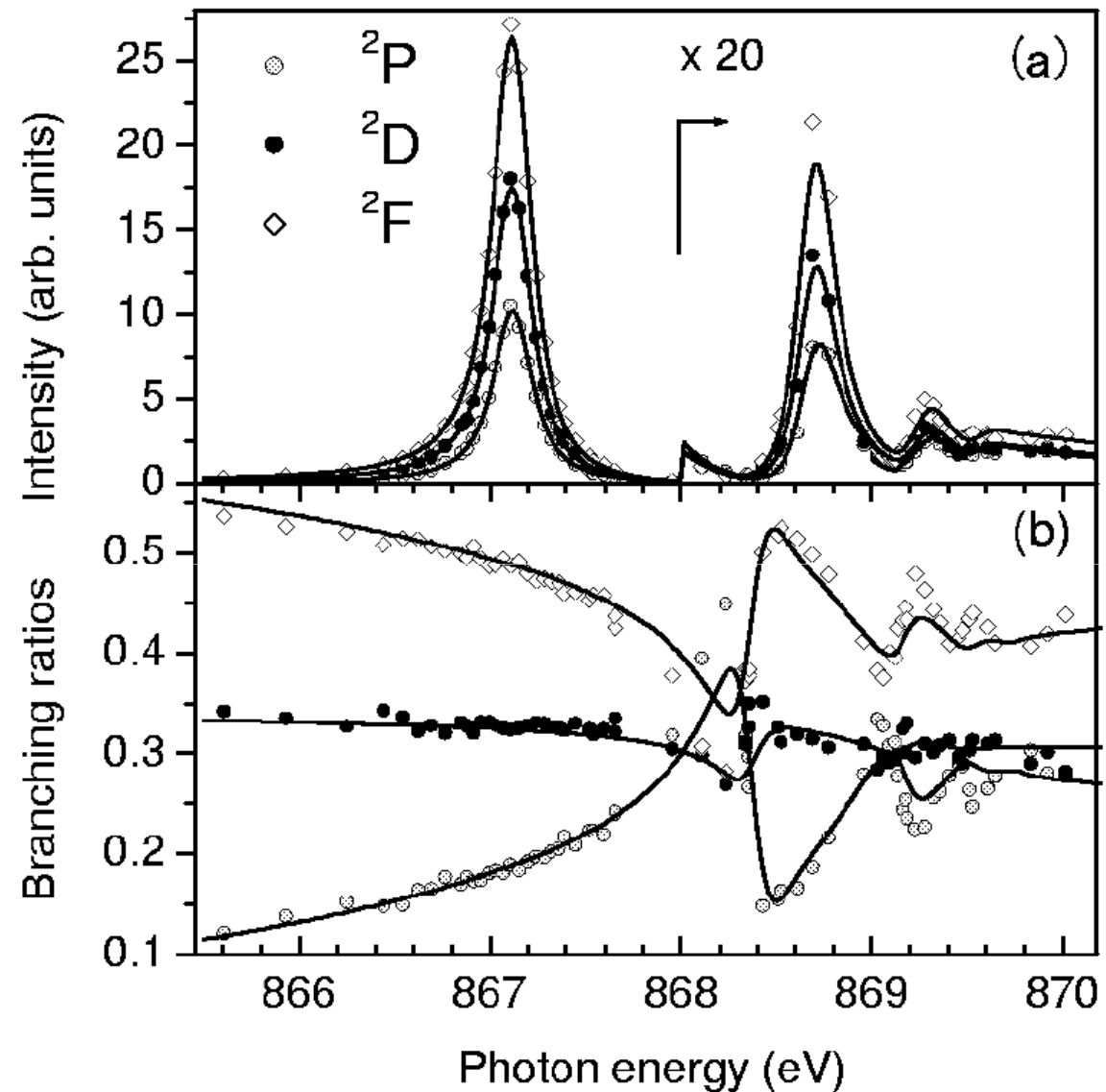
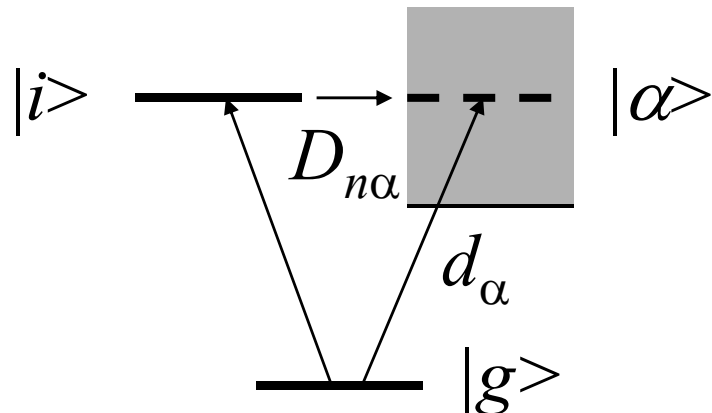
$$A_\alpha = d_\alpha + \sum_n \frac{D_{n\alpha}}{i + \varepsilon_n}$$

$$\sigma_\alpha = |A_\alpha|^2$$

$$\varepsilon_n = (h\nu - E_n) / (\Gamma_n / 2)$$

$$d_\alpha = \langle g | r | \alpha \rangle$$

$$D_{n\alpha} = \langle g | r | i_n \rangle \langle i_n | \alpha \rangle$$



De Fanis *et al.* Phys. Rev. Lett. **89**, 023006 (2002).

Sendai City



Jozenji Street



Statue of Load Date



Introduction of molecular world

$$H\Psi(R, r) = E\Psi(R, r) \quad H = T_R + T_r + V(r, R)$$

$$T_R = -\frac{\hbar^2}{2} \sum_k \frac{\partial^2}{M_k \partial R_k^2} \quad \text{KE of nucleus} \quad T_r = -\frac{\hbar^2}{2m} \sum_j \frac{\partial^2}{\partial r_j^2} \quad \text{KE of electrons}$$

$$H = H_0 + T_R \quad H_0 = T_r + V(r, R)$$

$$[H_0 - \varepsilon_n(R)]\varphi(R, r) = 0$$

$\varepsilon_n(R)$: adiabatic potential energy

$$\Psi(R, r) = \sum_n \Phi_n(R) \varphi_n(R, r)$$

$$\int \varphi^*(R, r)(H - E)\Psi(R, r)dr = 0$$

$$[T_R + \varepsilon_m(R)]\Phi_{mv}^0(R) = E_{mv}^0 \Phi_{mv}^0(R)$$

Nuclear motion is within the adiabatic potential energy surface!

Born-Oppenheimer approximation

Franck-Condon approximation for photoionization

$$\sigma_{iv'}^+(E) \sim |\int X_{iv'}^*(R) D_E(R) X_0(R) dR|^2$$

$X_{iv'}^*(R), X_0(R)$: Vibrational wavefunctions of ionic iv' and ground 0 states

$$D_E(R) = \int \varphi_E^*(r, R) r \varphi_{\text{core}}(r, R) dr$$

$\varphi_E(r, R), \varphi_{\text{core}}(r, R)$: Electronic wavefunctions of the continuum E and core orbitals

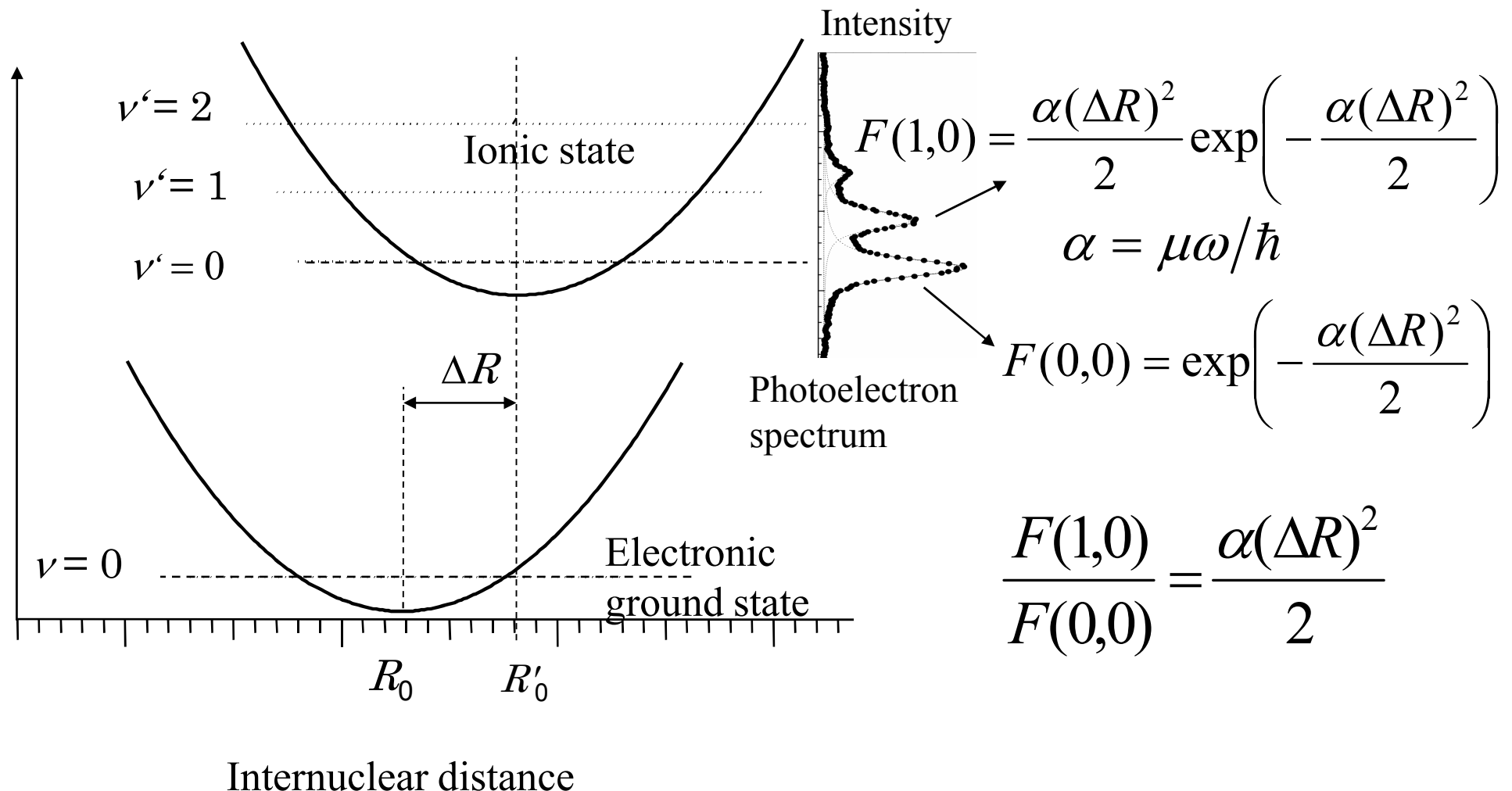
Assume that the dipole moment $D_E(R)$ does not depend on R

$$\sigma_{iv'}^+(E) \sim |D_E(R_e)|^2 F(v'0)$$

$$F(v'0) = |\int X_{iv'}^*(R) X_0(R) dR|^2 \quad \text{Franck-Condon factor}$$

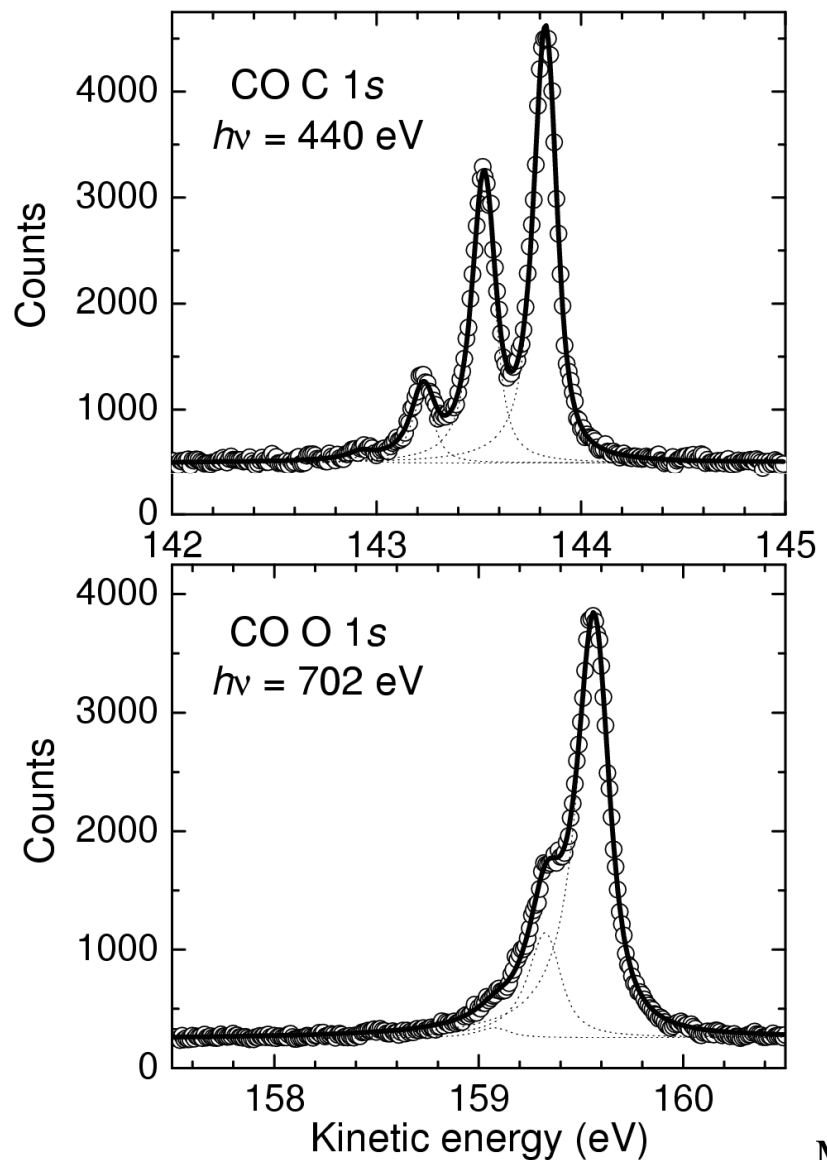
Vibrational intensity distribution in the photoelectron spectrum is determined by the Franck-Condon factors

Franck-Condon analysis based on harmonic approximation Linear coupling model



One can extract ΔR from photoelectron spectroscopy!

Franck-Condon analysis for the vibrational structure of the C 1s and O 1s mainlines of CO



$I \sim |\langle \psi_v^+ | \psi_0 \rangle|^2$: FC factor

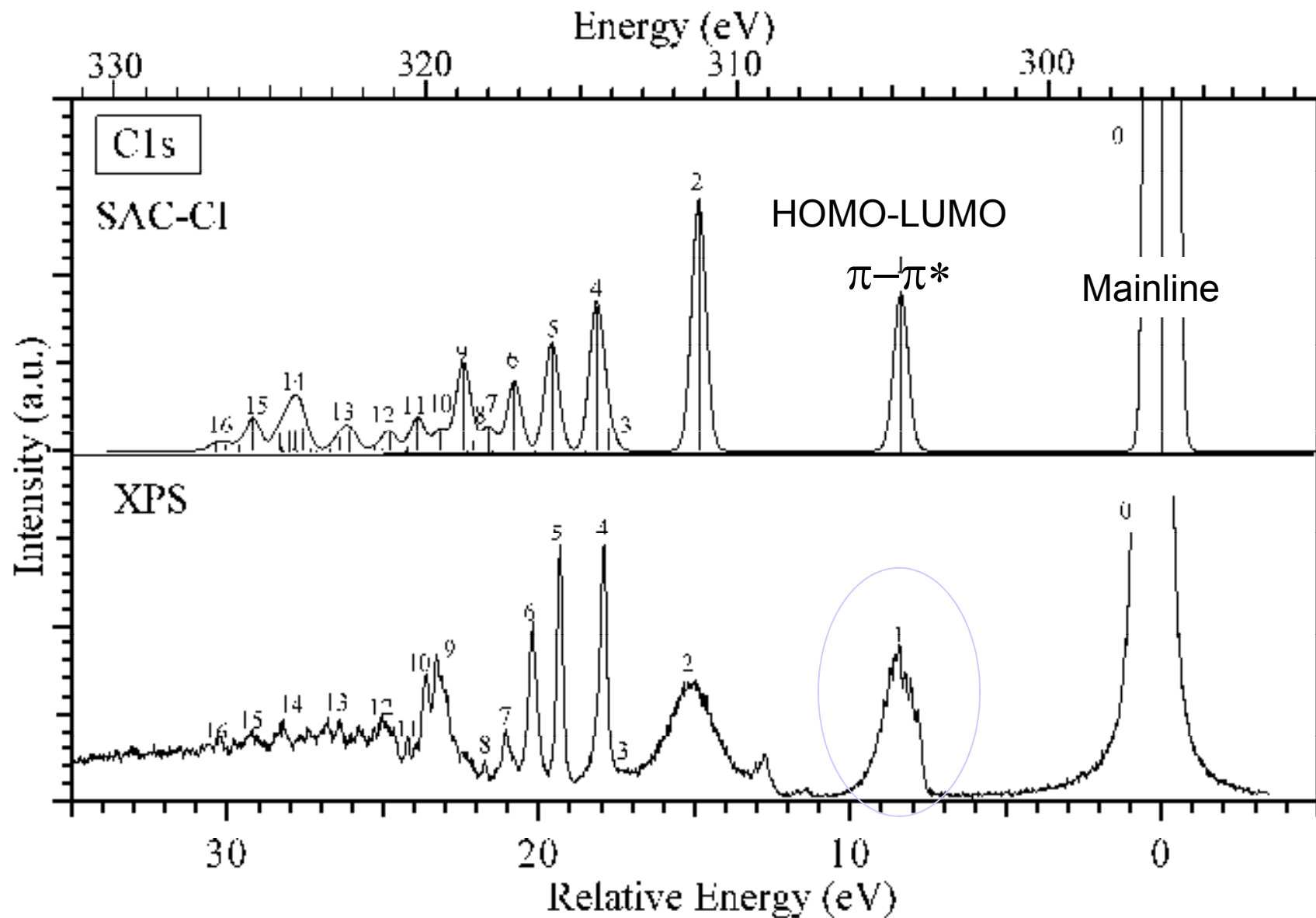
ψ_0 : v=0 vibrational wave function in the ground state

ψ_v^+ : v-th vibrational wave function in the core-ionized state

Stable geometry of the core-ionized state extracted from the vibrational structure

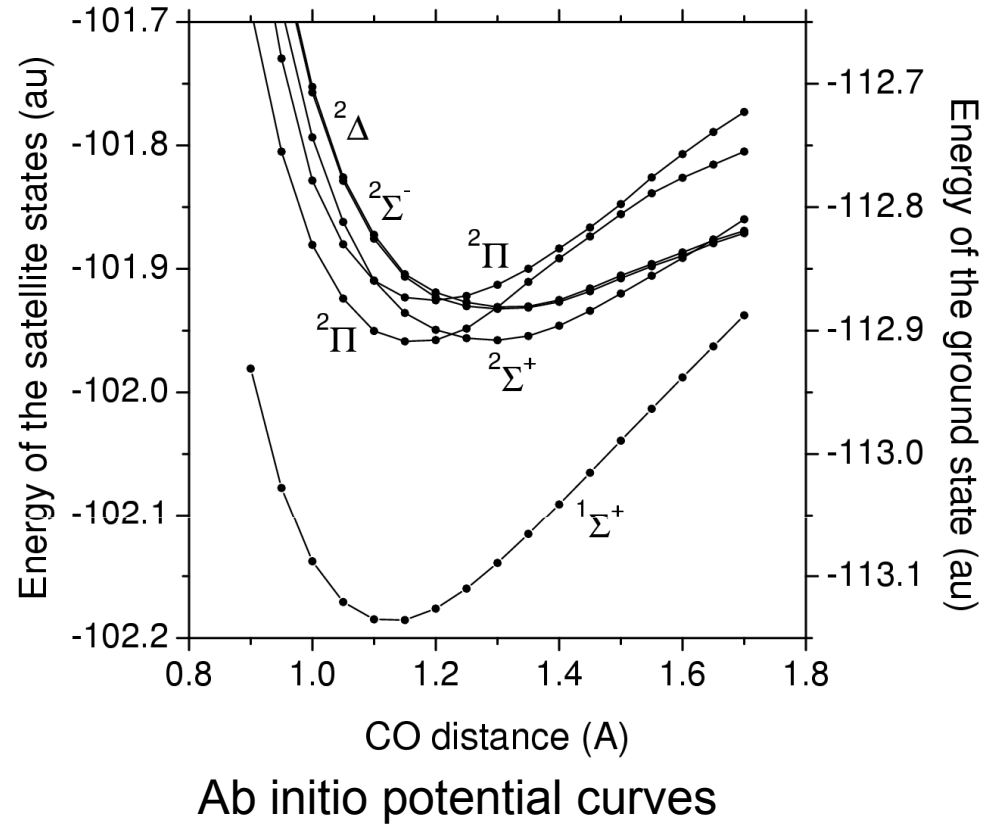
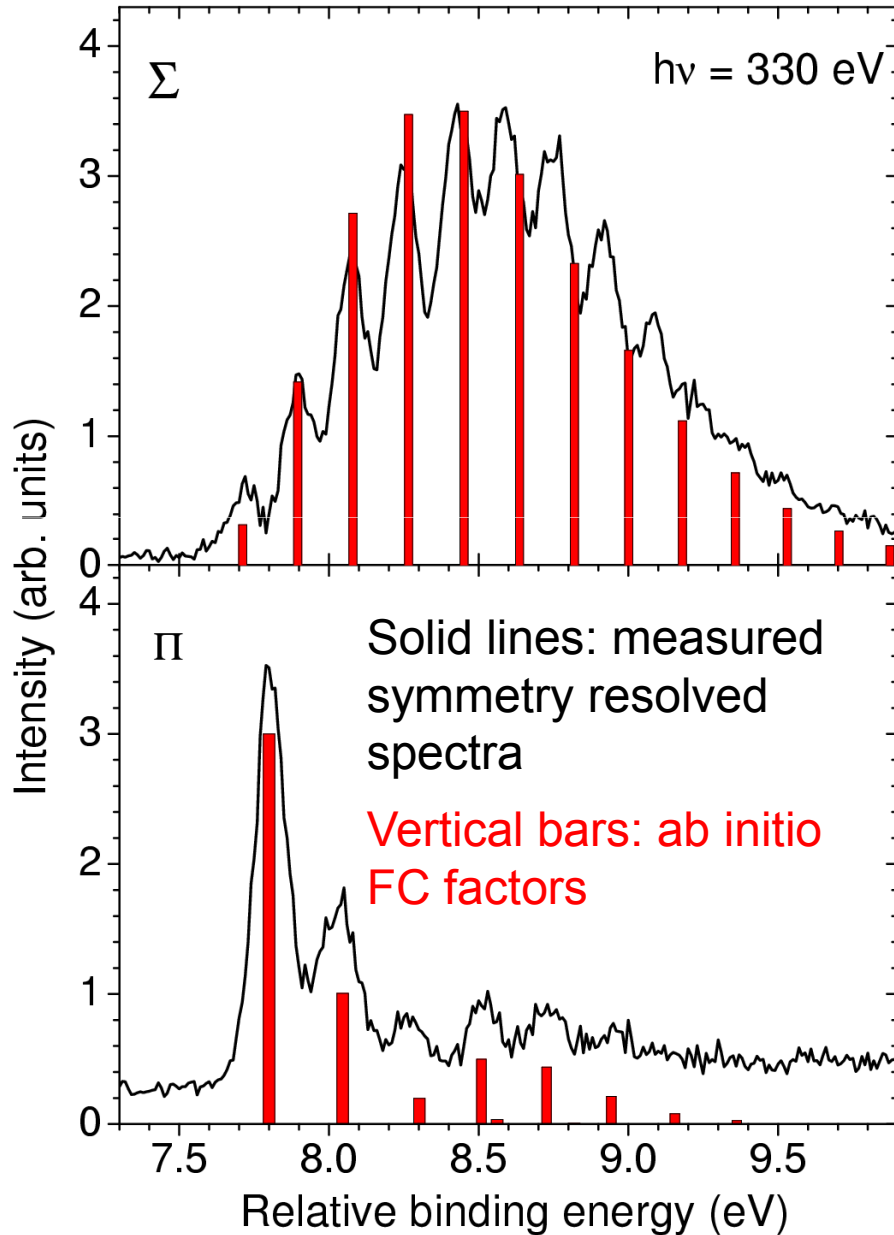
	Exper.	Theory
$C\ 1s^{-1}$		
$\Delta R_e (\text{\AA})$	-0.051 (1)	-0.051
$O\ 1s^{-1}$		
$\Delta R_e (\text{\AA})$	0.037(2)	0.028

Satellite spectrum in core-level photoemission in CO



Ehara *et al.* J. Chem. Phys. **125**, 114304 (2006).

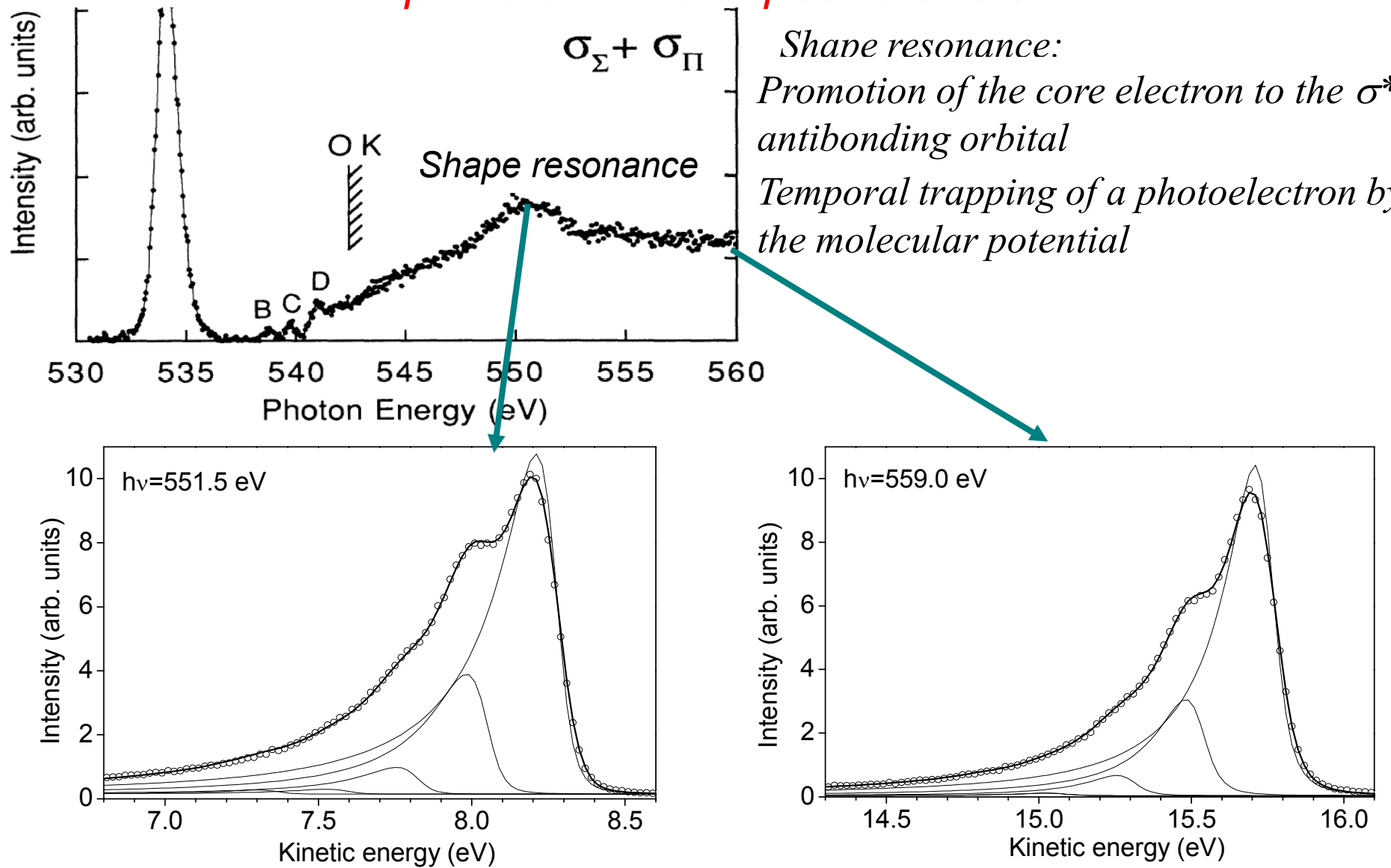
Franck-Condon analysis of the vibrational structure in the symmetry-resolved C 1s satellite bands of CO



Ab initio FC factors reproduce the measured vibrational distributions.

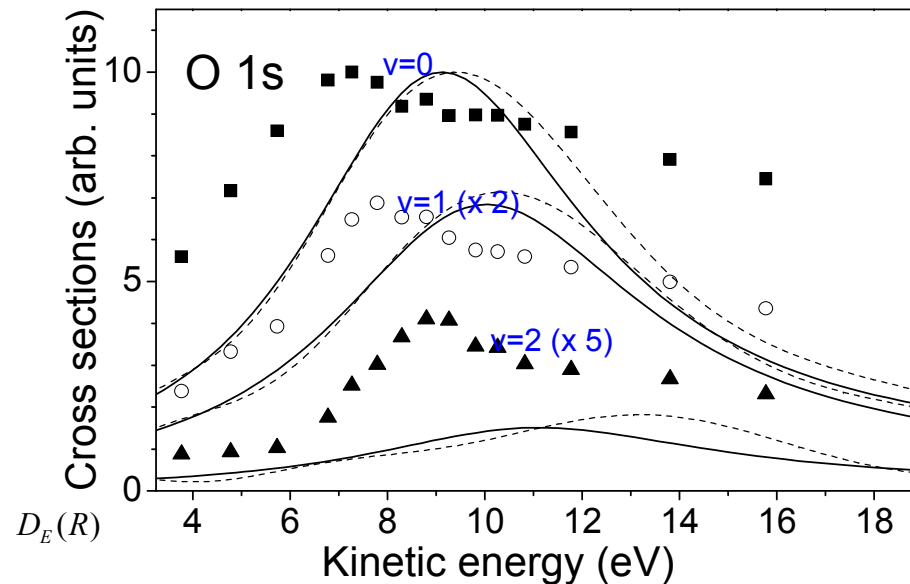
Ueda *et al.*, Phys. Rev. Lett. **94**, 243004 (2005).

Vibrational effects on the shape resonance energy in the K-shell photoionization spectra of CO



O 1s photoelectron spectra of CO at the shape resonance and far above it.
Non-Franck-Condon behavior of vibrational distributions!

Vibration-dependent shape resonances



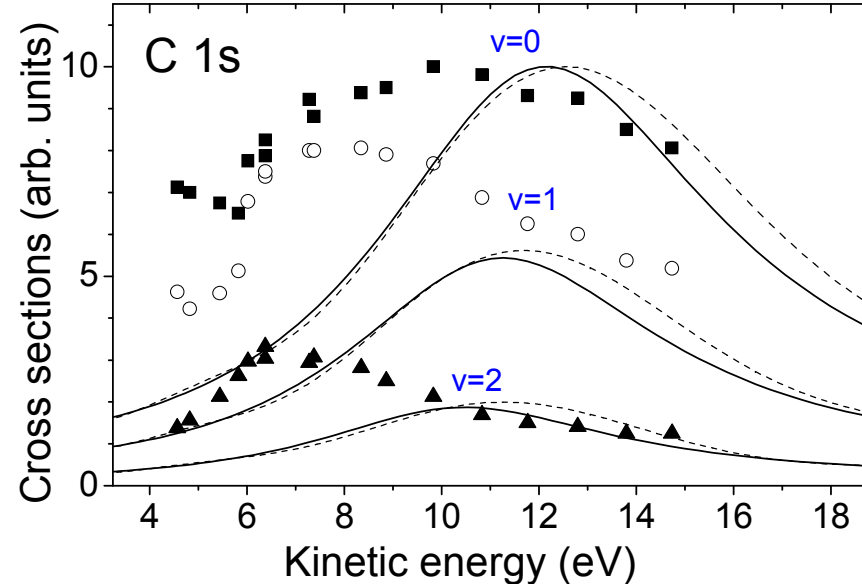
Shape resonance energy increases with v' .

D. A. Mistrov *et al.* Phys. Rev. A **68**, 022508 (2003).

$$\sigma_{iv'}^+(E) \sim \left| \int X_{iv'}^*(R) D_E(R) X_0(R) dR \right|^2 , \quad D_E(R) = \int \varphi_E^*(r, R) r \varphi_{\text{core}}(r, R) dr$$

$D_E(R)$ strongly depends on R in the shape resonance region!

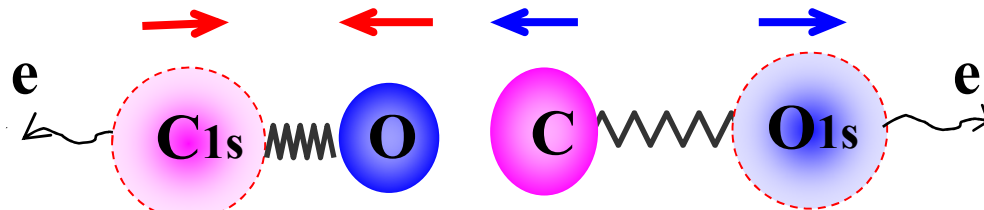
J. L. Dehmer, D. Dill, and S. Wallace, *Phys. Rev. Lett.* **43**, 1005 (1979).



Shape resonance energy decreases with v' .

K. J. Randall *et al.*, Phys. Rev. Lett. **71**, 1156 (1993).

Origin of the vibrational energy on the shape resonance energy



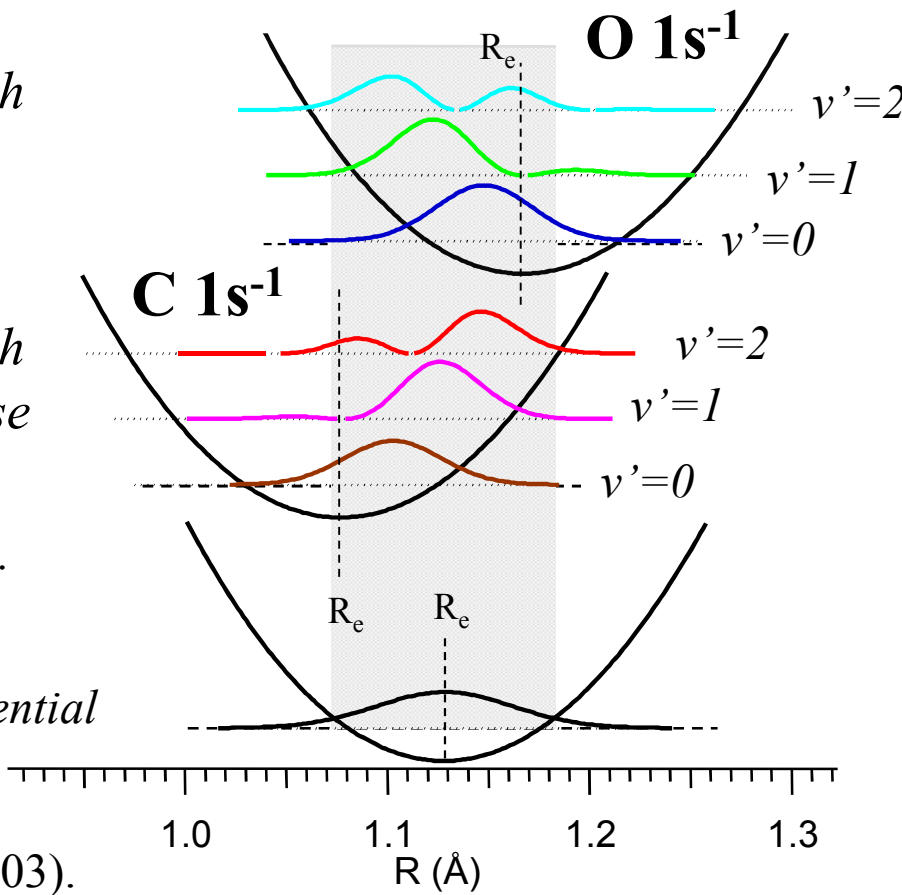
Characteristic bond length shrinks with the increase in v' for O 1s.

Characteristic bond length elongates with the increase in v' for C1s.

Shape resonance formation:

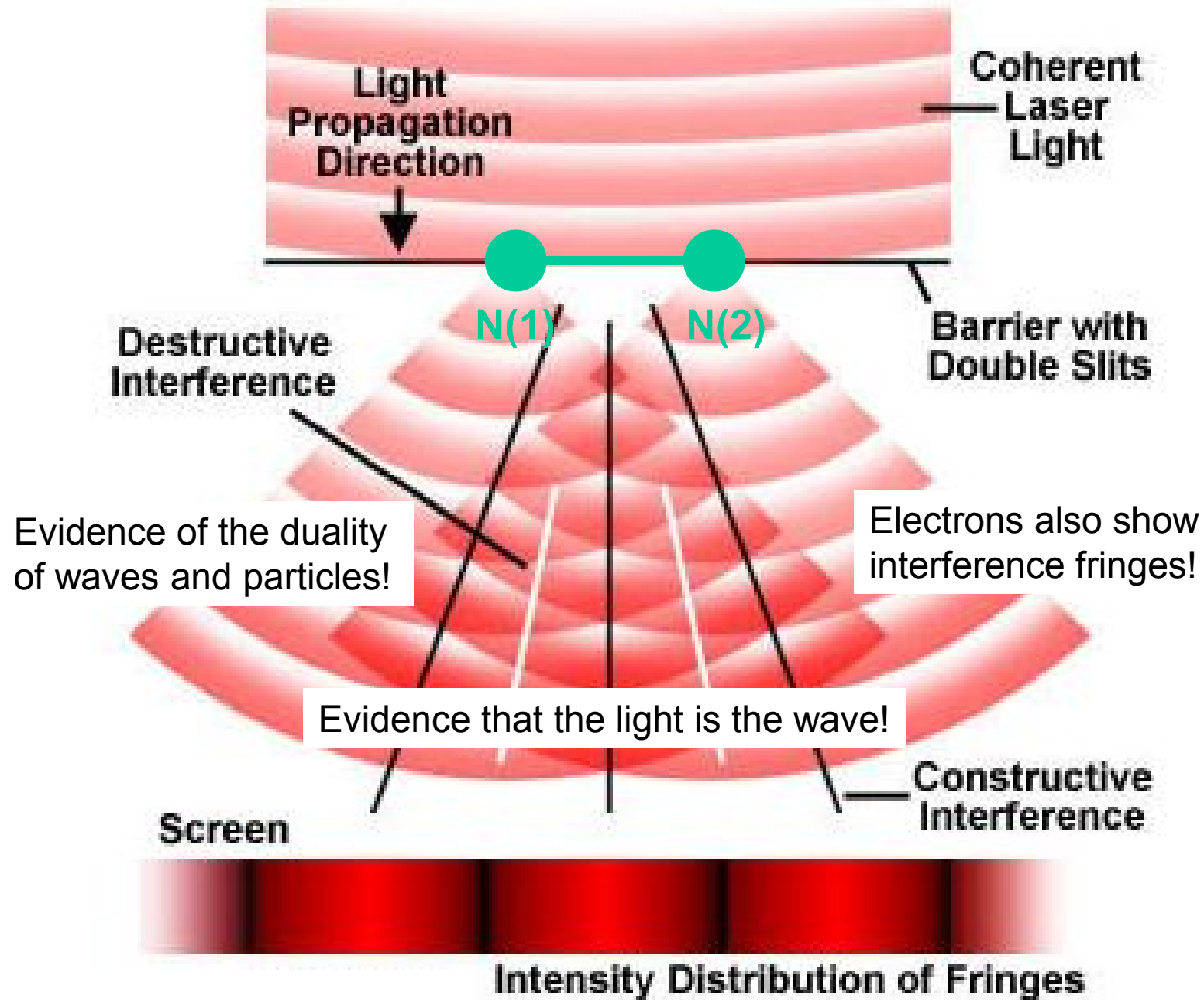
$$kR + \varphi = \pi$$

Cf. standing wave in the box potential

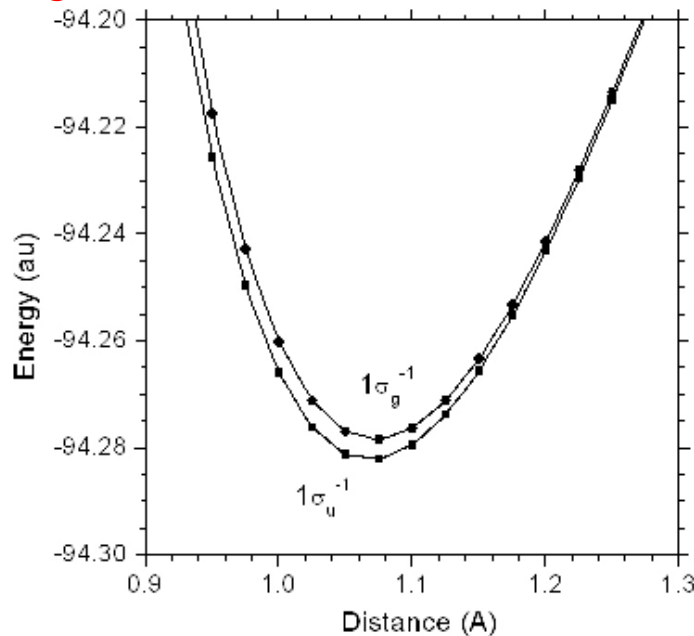
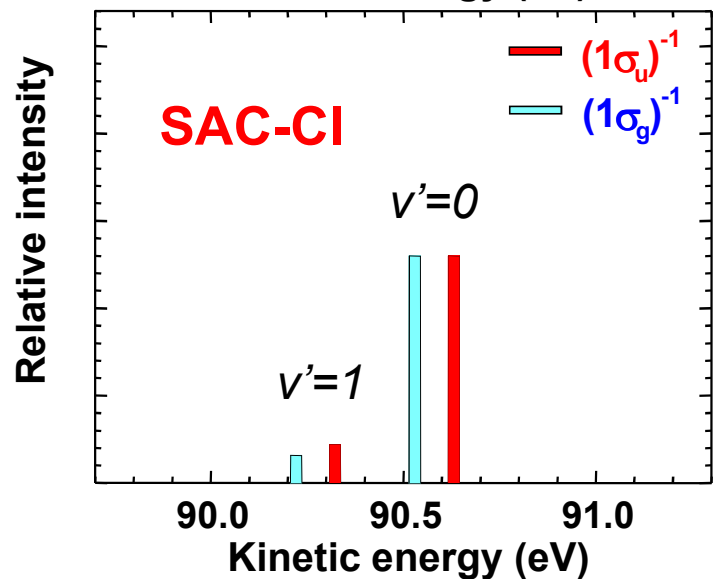
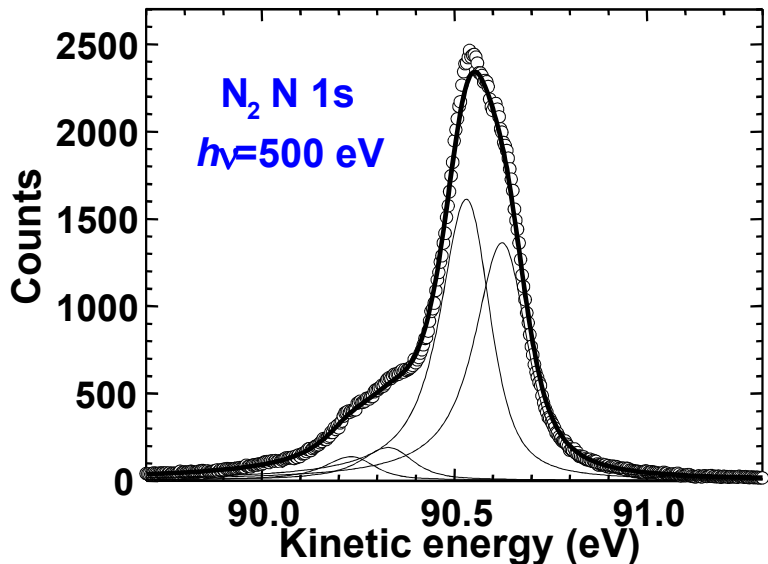


D. A. Mistrov *et al.*
Phys. Rev. A **68**, 022508 (2003).

Young's Double Slit Experiment



Franck-Condon analysis for the vibrational structure of the N 1s $1\sigma_u$ and $1\sigma_g$ mainlines of N_2



Equilibrium geometries of the core-ionized states extracted from the vibrational structure

	Exper.	Theory
$N\ 1\sigma_u^{-1}$		
ΔR_e (Å)	-0.023(1)	-0.021
$N\ 1\sigma_g^{-1}$		
ΔR_e (Å)	-0.018(1)	-0.017

Ehara *et al.* JCP **124**, 124311 (2006)

Cohen-Fano two-center interference

Two 1s orbitals in N_2 correspond to Young's double slits.

Molecular core-level orbitals: $1\sigma_{g,u} = \frac{1s_1 \pm 1s_2}{\sqrt{2}}$.

Core-level photoemission from fixed-in-space N_2 :

$$\sigma_{g,u}(\omega) \propto \frac{1}{2} |e^{ik \cdot R_1} \pm e^{ik \cdot R_2}|^2 = 1 \pm \cos(k \cdot R),$$

.....
Two center photoelectron wave *Interference fringe*

where k : photoelectron momentum; R_1, R_2 : position vectors of N (1) and N(2)
 $\vec{R} = \vec{R}_1 - \vec{R}_2$.

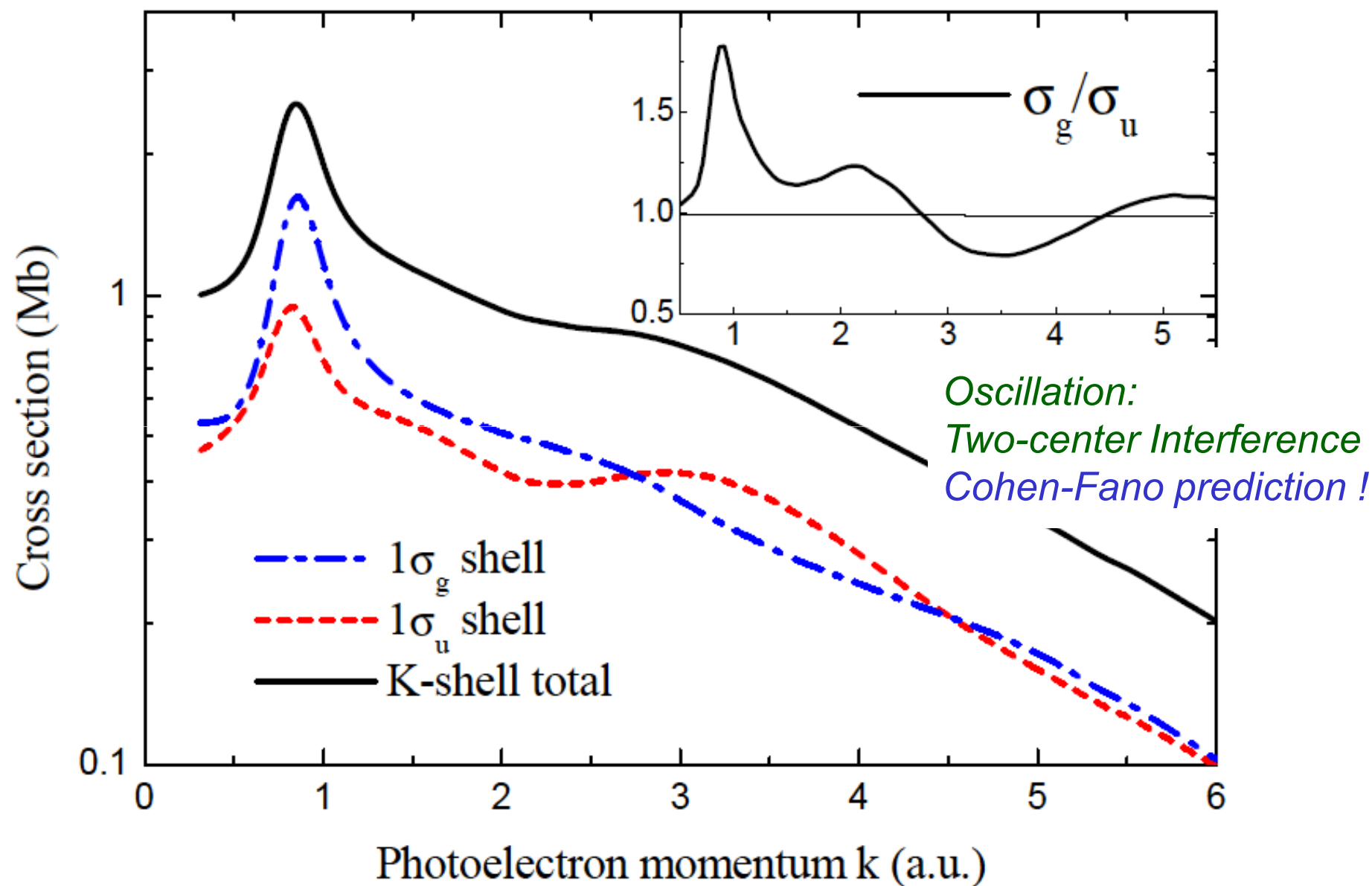
Orientational average: Cohen-Fano formula

$$\sigma_{g,u}(\omega) = \sigma_0(\omega) [1 \pm \chi_{CF}(k)], \quad \chi_{CF}(k) = \frac{\sin kR}{kR}$$

Interference oscillatory structure becomes much smaller but remains!

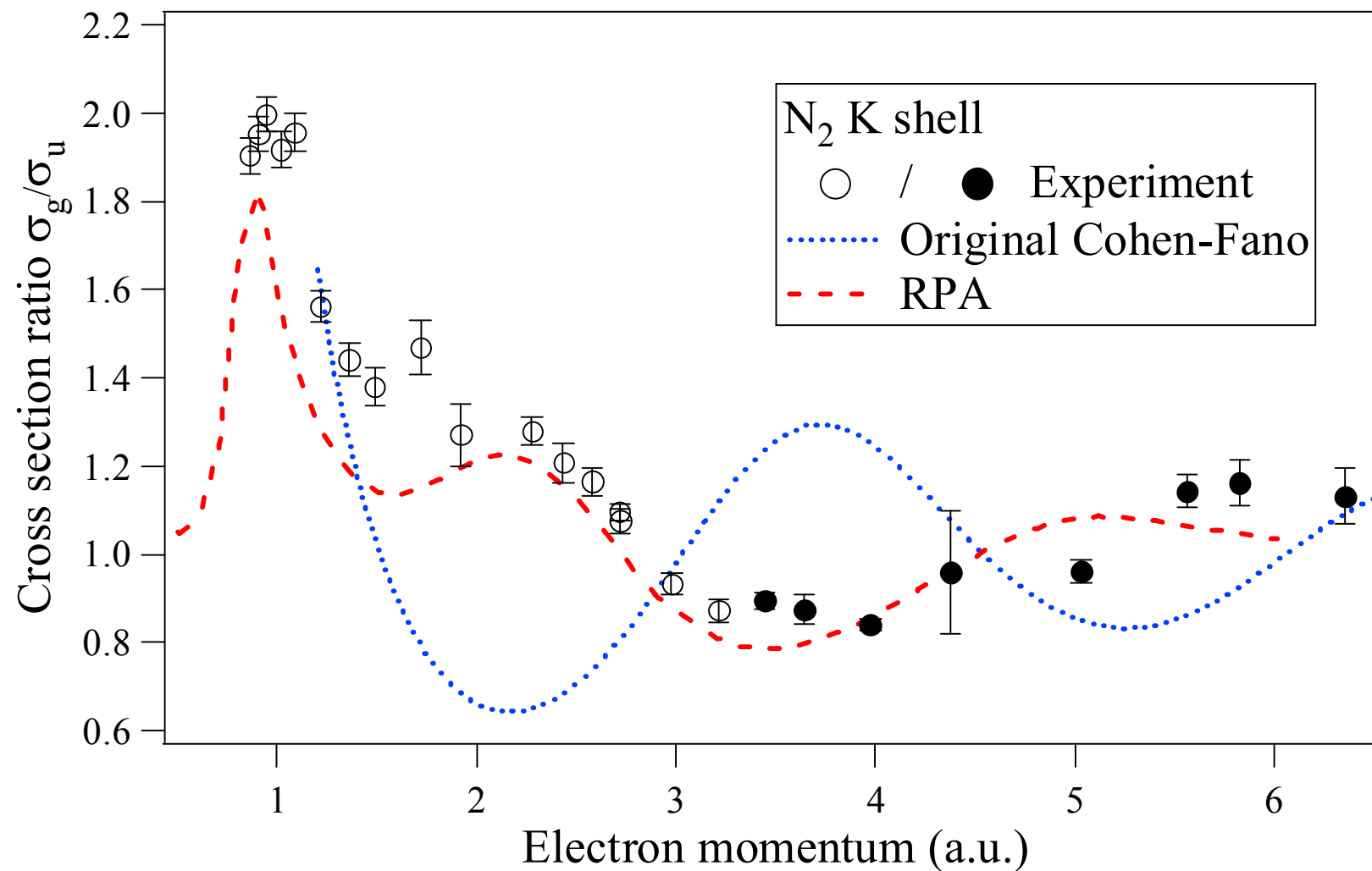
H.D. Cohen and U. Fano, Phys. Rev. **150**, 30 (1966).

Ab initio N 1s $1\sigma_u$ and $1\sigma_g$ photoionization cross sections of N_2



Semenov *et al.*, J. Phys. B: At. Mol. Opt. Phys. 39, L261 (2006)

σ_g/σ_u ratio: experiment vs ab initio and Cohen-Fano



Both experimental and ab initio interference fringes shift from the prediction by Cohen-Fano formula!

Liu *et al.*, J. Phys. B. **39**, 4801-4817 (2006); JESRP **156-158**, 73-77 (2007).

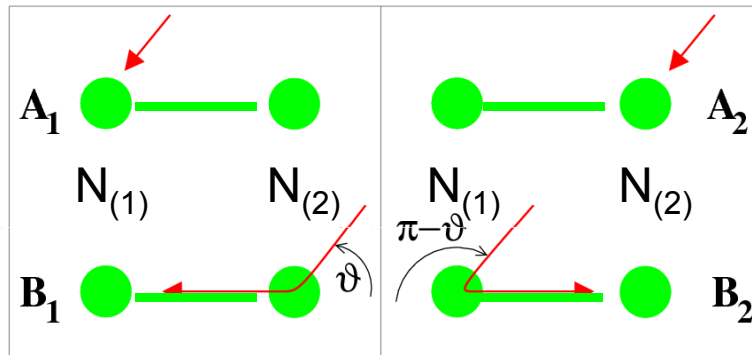
Photoelectron scattering by the neighboring N atom

The amplitude of the photoelectron wave from one center:

$$\psi_1 = \frac{\hat{k}e^{ik \cdot R_1}}{A_1} + \frac{\hat{R} \frac{e^{ikR}}{R} f(\vartheta) e^{ik \cdot R_2}}{B_1}.$$

$$\psi_2 = A_2 + B_2$$

The amplitude of the photoelectron wave from two centers: $\psi_1 \pm \psi_2$



Cohen-Fano interference
A₁A₂ interference term

$$\chi_{CF}(k) = \frac{\sin kR}{kR}$$

The cross section $\sim |\psi_1 \pm \psi_2|^2 = |(A_1 + B_1) \pm (A_2 + B_2)|^2$

$$\frac{\sigma_{g,u}(\omega)}{\sigma_0(\omega)} = 1 - \frac{1}{kR^2} \text{Im} \left\{ f(\pi) e^{2i[kR + \delta_1(k)]} \right\} \pm \chi(k),$$

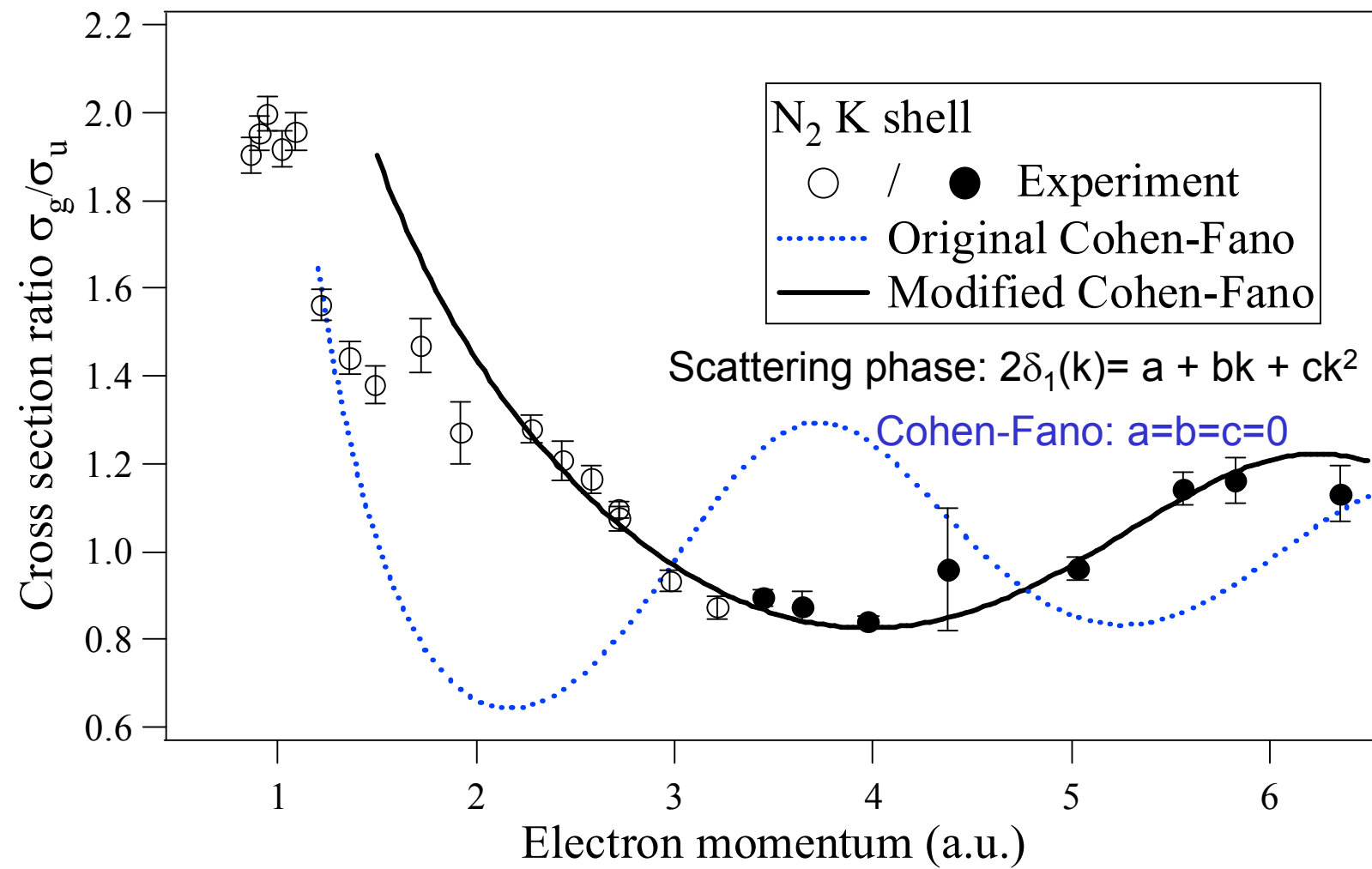
A₁B₁ and A₂B₂ one-center interference terms

$$\chi(k) = \frac{1}{kR} \sin [kR + 2\delta_1(k)] \quad \delta_1(k): \text{scattering phase}$$

CF A₁A₂ interference term

A₁B₂ and A₂B₁ two-center interference terms !

σ_g/σ_u ratio fitted by modified Cohen-Fano



Fitted results: $a = -5.2 \pm 0.6$, $b = -1.6 \pm 0.4$, $c = 0.09 \pm 0.05$ a.u.

Ab initio results: $a = -4.8$, $b = -1.15$, $c = 0.069$ a.u.

(Teo and Lee, J. Am. Chem. Soc. **101**, 2815 (1979))

Near Sendai

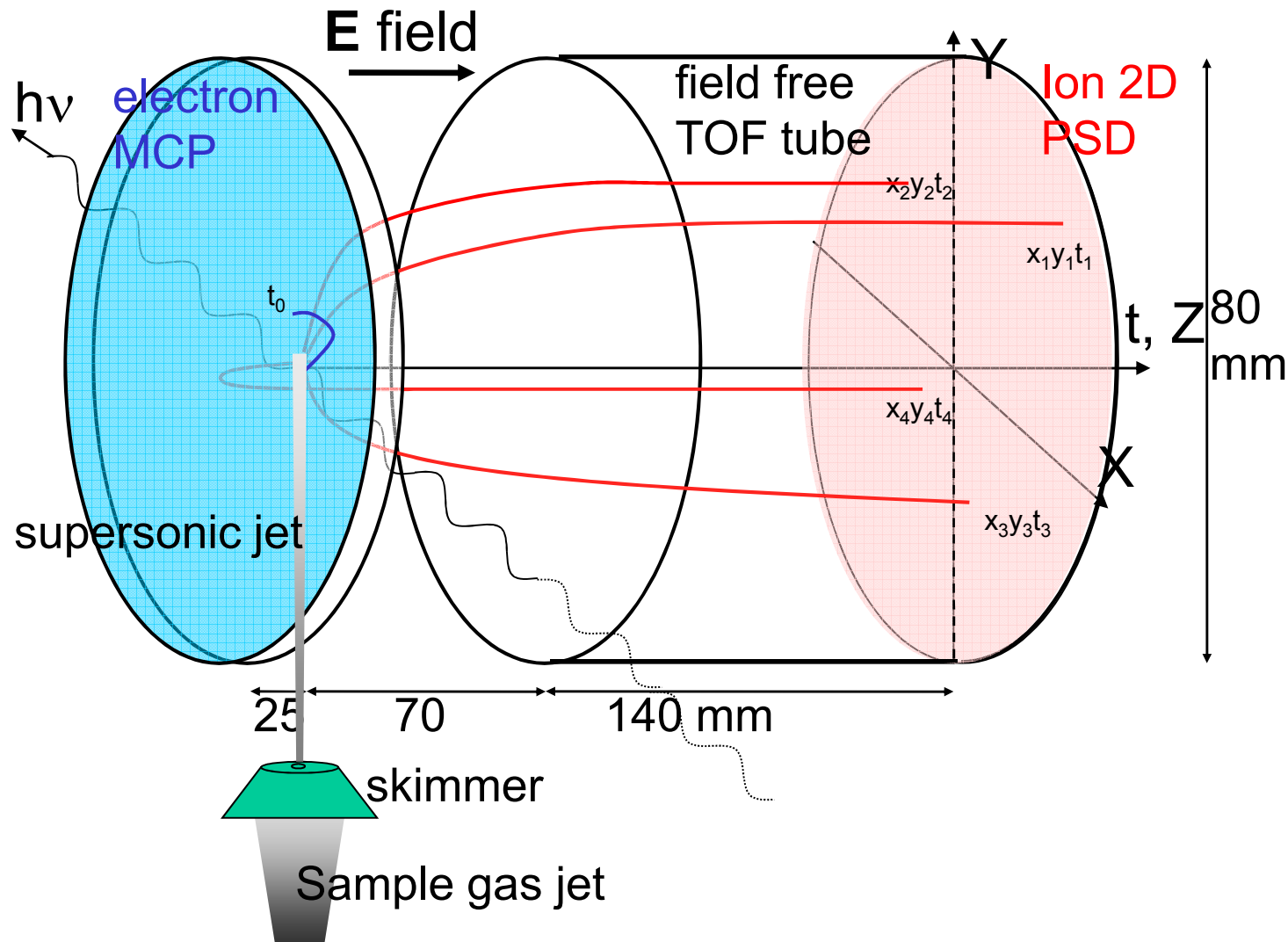


Motsu-ji



Chuson-ji

Multiple-ion coincidence imaging setup



position & time of flight (x, y, t)



3D momentum of each particle

How to obtain 3D momentum

$$p_x = \frac{m(x - x_0)}{t}, \quad p_y = \frac{m(y - y_0)}{t}, \quad p_z = qE(t - t_0)$$

t: ion time-of-flight

t_0 : ion TOF at rest

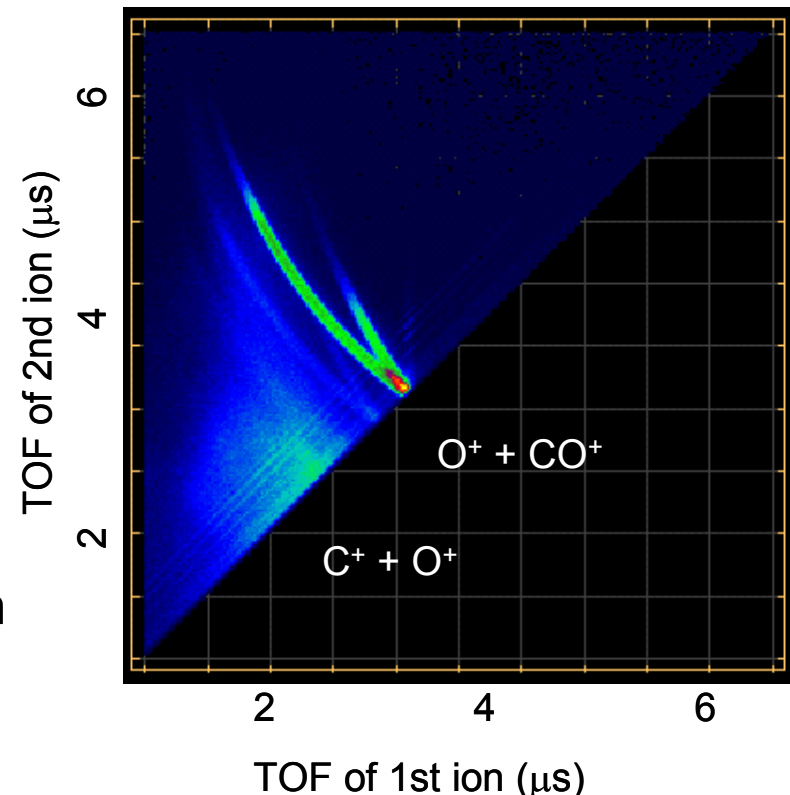
x, y: arrival position on the detector.

x_0, y_0 : initial position of the ion

m : ion mass

q: ion charge

E: electric field in the acceleration region



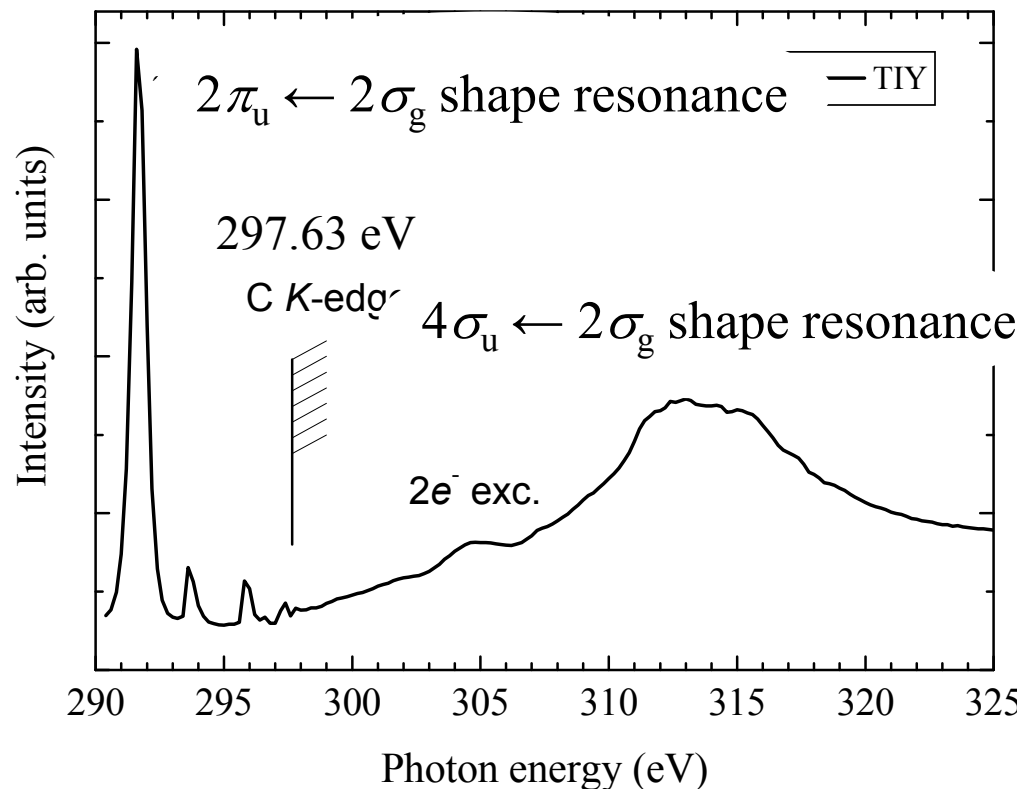
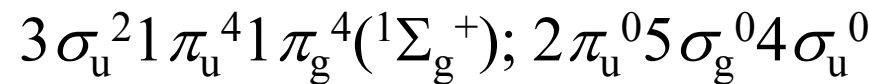
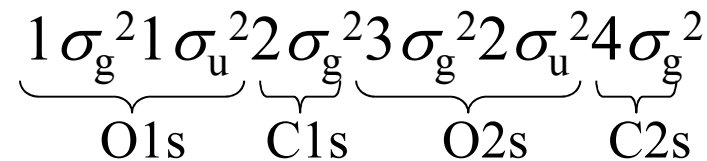
To be exact P_z becomes nonlinear



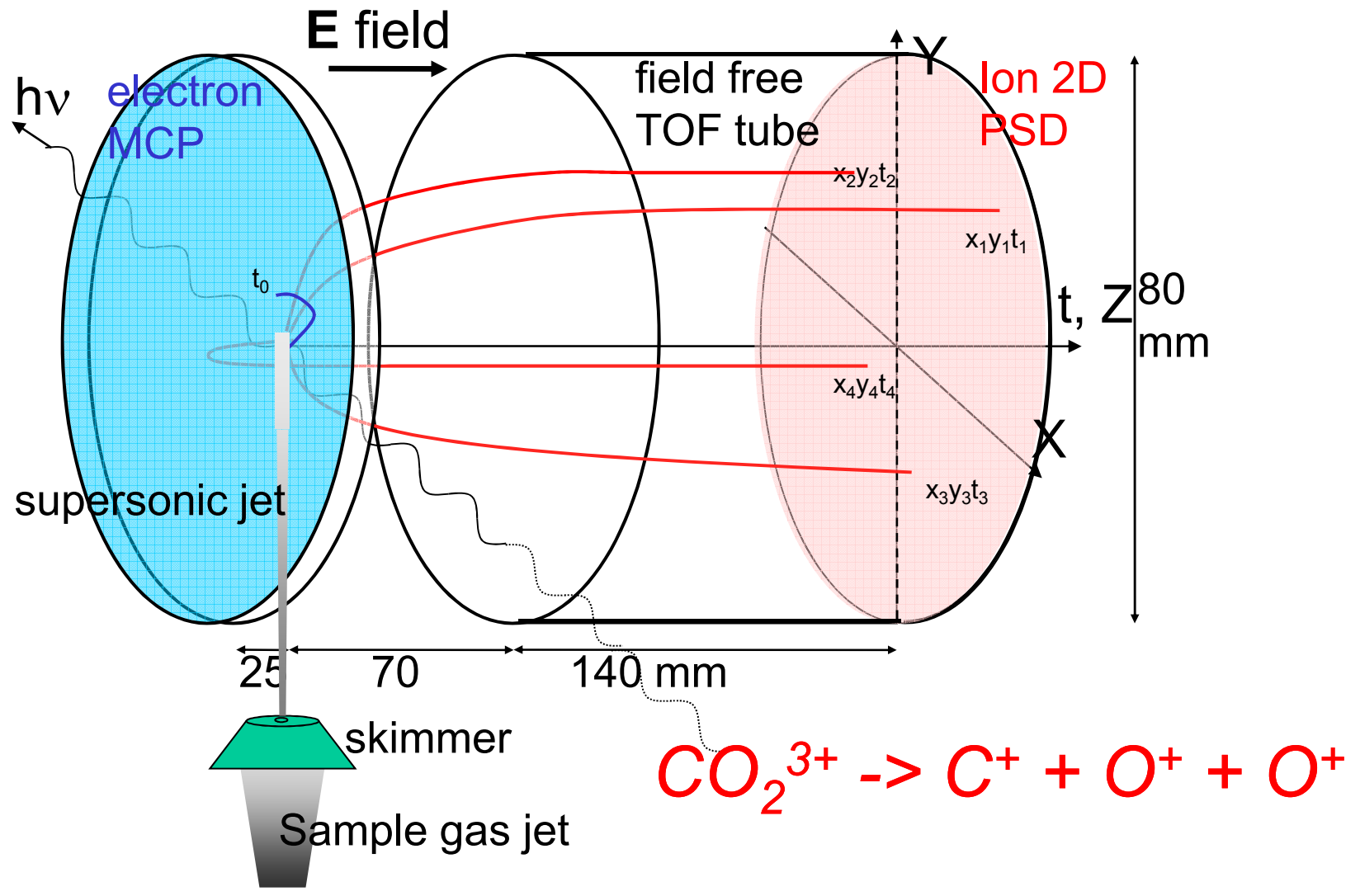
Iterative procedure

Total electron yield spectrum of CO₂ in the C1s ionization region

CO₂ ground state configuration:

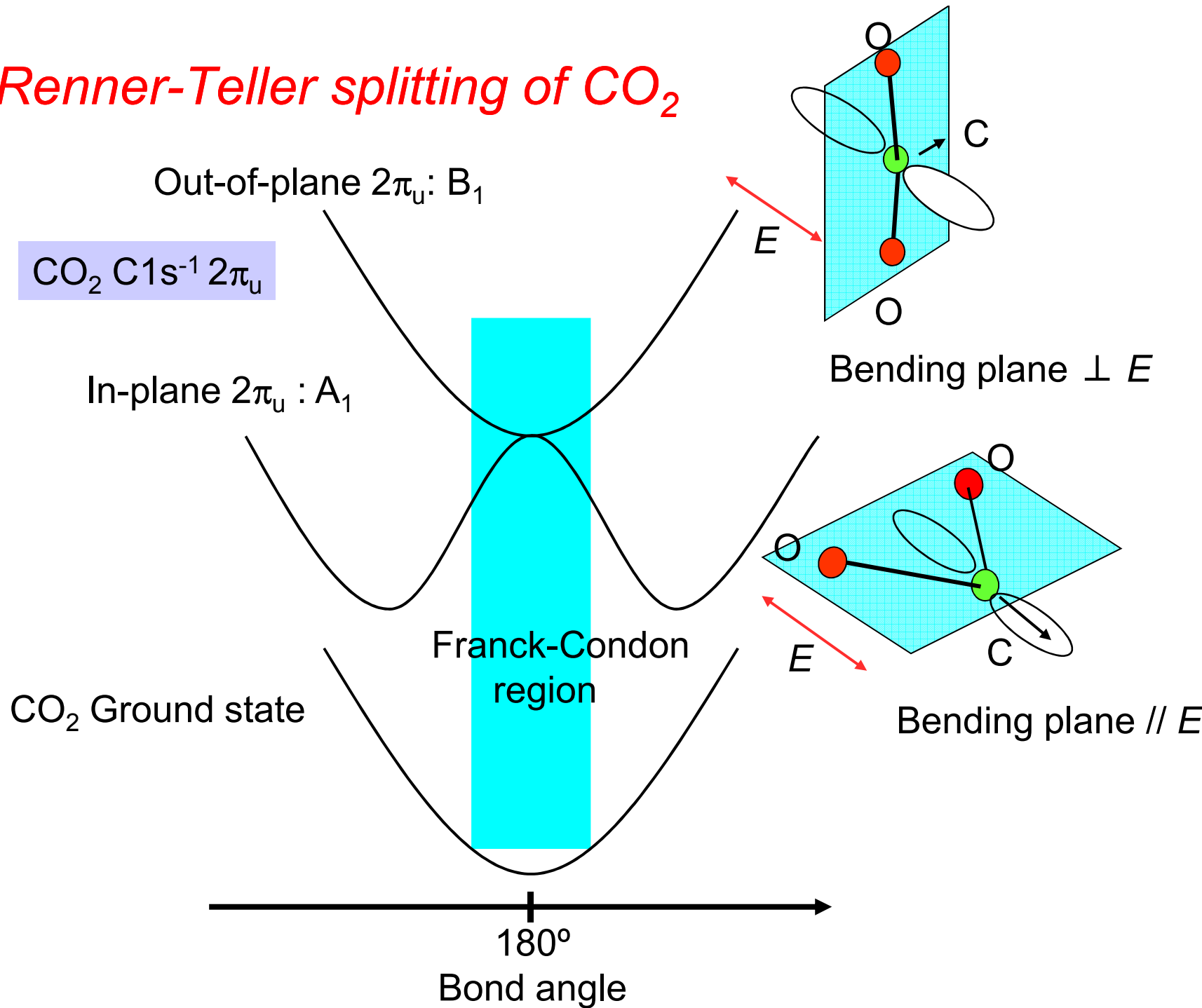


SR experiments with multiple-ion coincidence

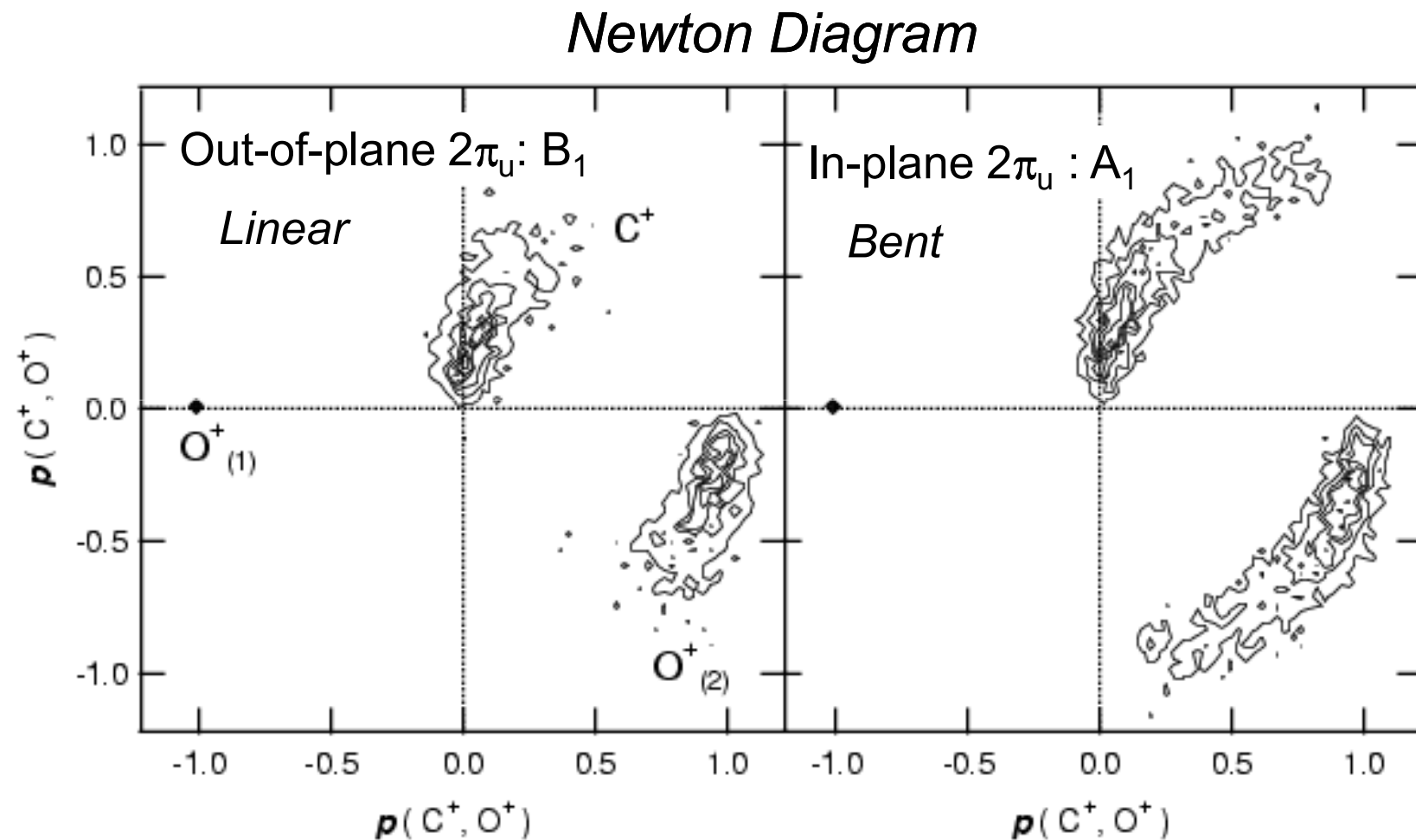


position & time of flight (x,y,t) → *3D momentum of each particle*

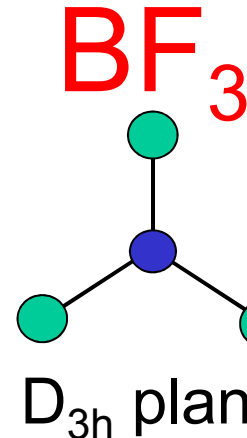
Renner-Teller splitting of CO_2



*Snapshot of the bending motion in the core-excited state
with a lifetime ~ 7 fs*



Muramatsu et al. Phys. Rev. Lett. 88, 133002 (2002).

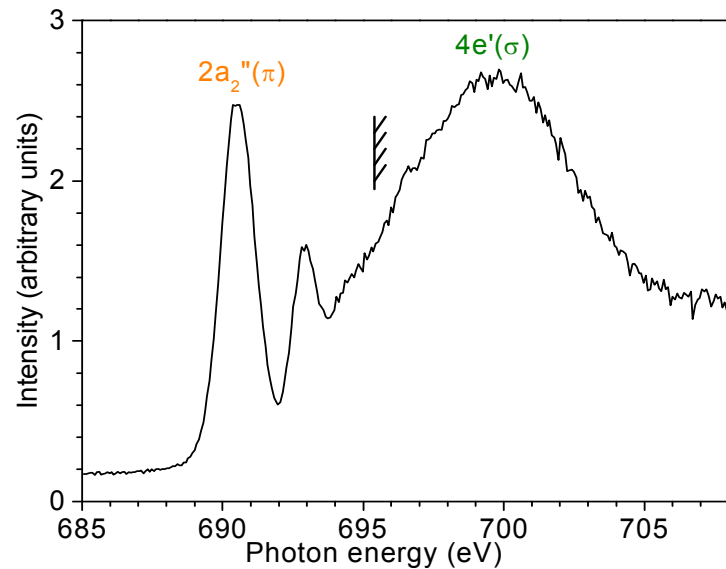


KK (1a₁')²(1e')⁴(2a₁')²(2e')⁴(1a₂")²(3e')⁴(1e")⁴(1a₂')²; (2a₂")⁰(4e')⁰

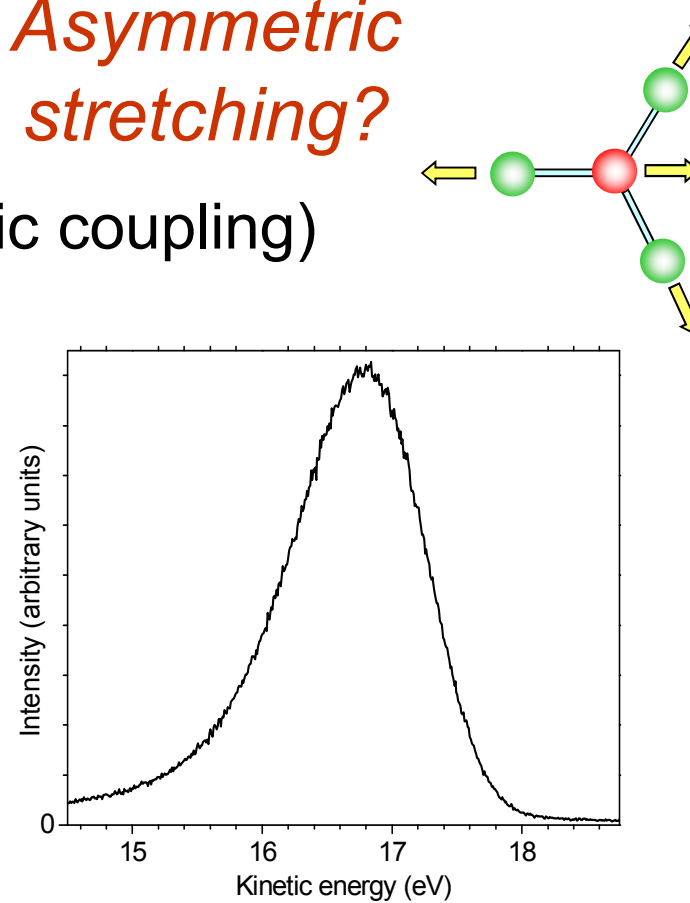
inner valence outer valence empty

F, B 1s

F 1s excitation/ionization
Symmetry breaking (due to vibronic coupling)

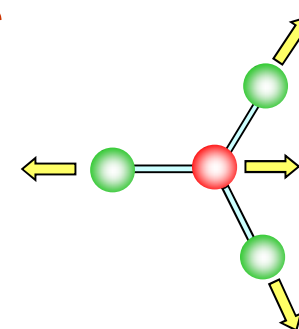


F1s excitation spectrum

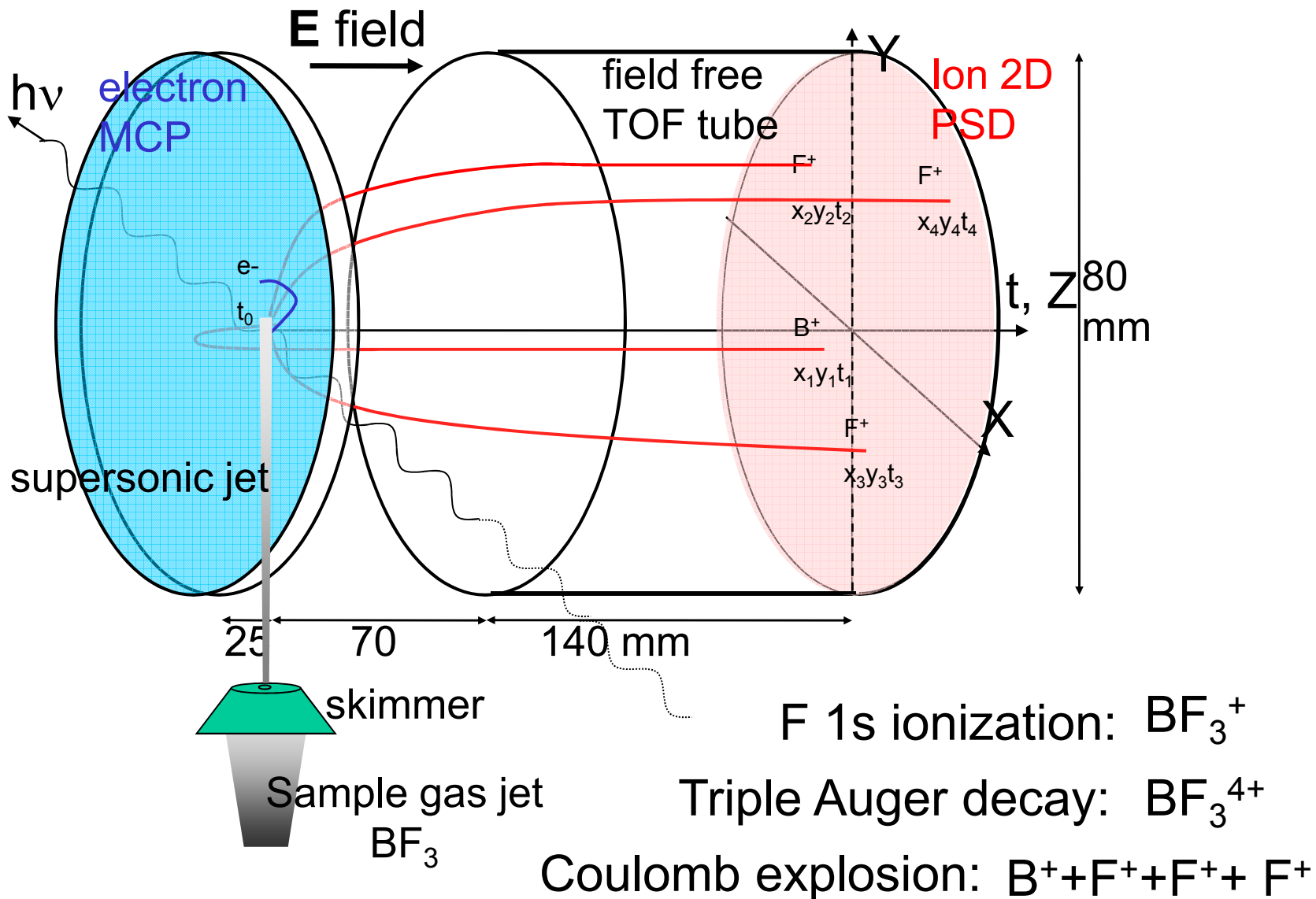


F1s photoelectron spectrum

Asymmetric stretching?



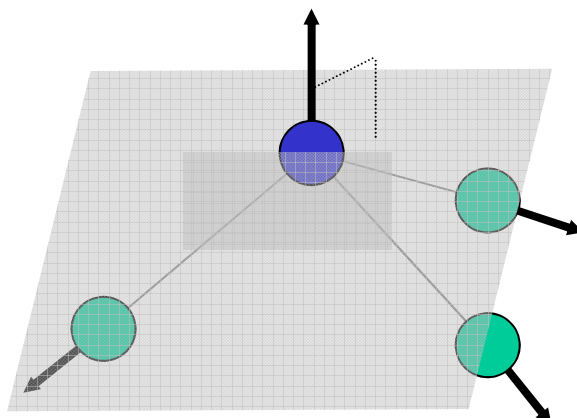
Multiple ion coincidence momentum imaging



Construction of Dalitz plots for $F^+ F^+ F^+$ in the plane perpendicular to $P(B^+)$

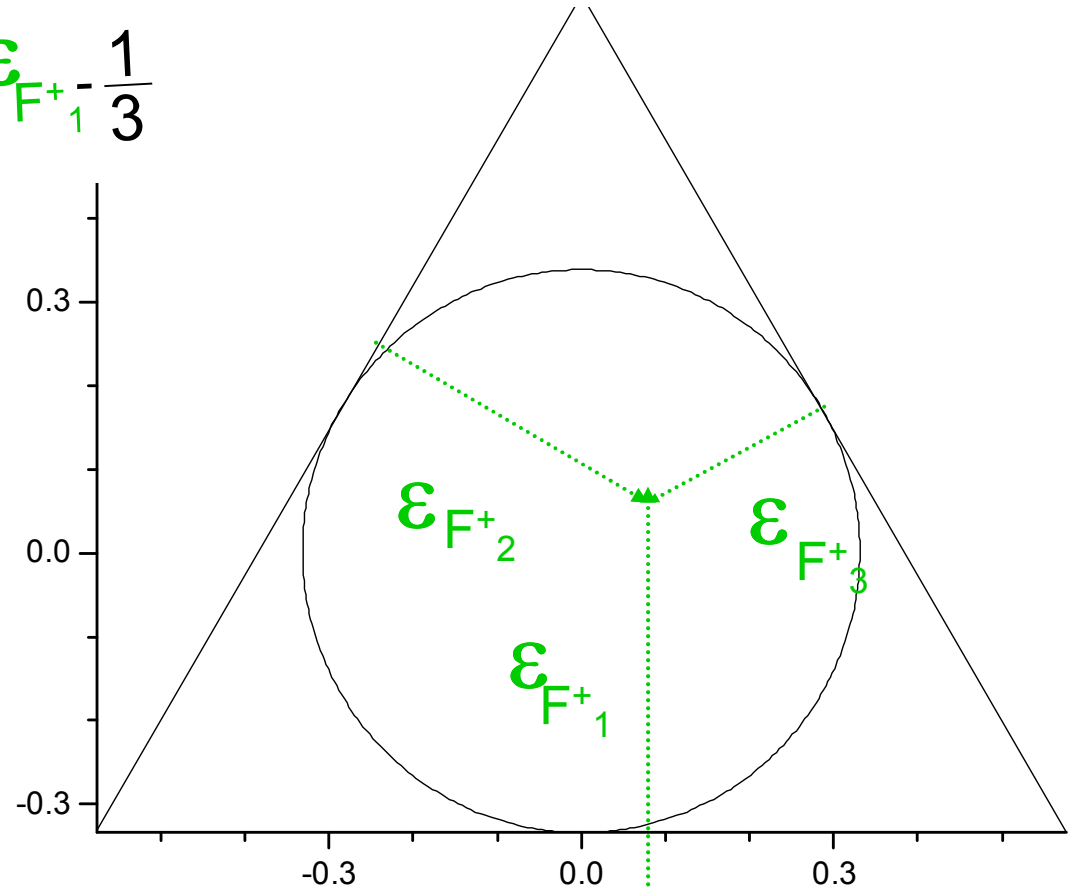
$$Y_D = \frac{\epsilon_{F^+_1} - \frac{1}{3}}{3}$$

$P_{F^+_i}$ are the projections
of momenta on the
plane perpendicular to
the emission of B^+



$$\epsilon_{F^+_i} = \frac{P_{\perp F^+_i}^2}{\sum P_{\perp F^+_i}^2}$$

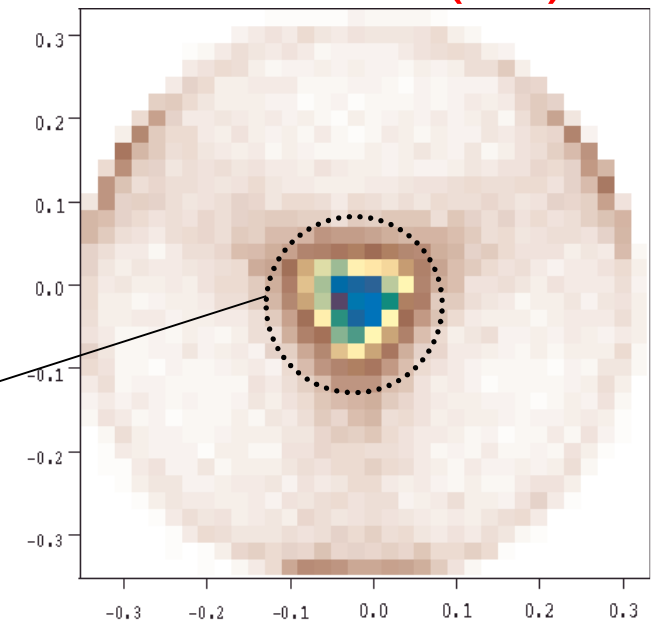
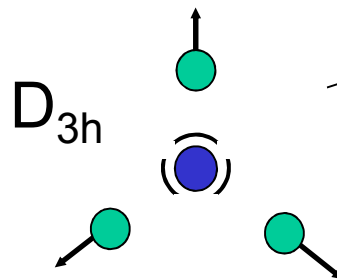
$$X_D = \frac{\epsilon_{F^+_3} - \epsilon_{F^+_2}}{3^{1/2}}$$



Motion of F⁺ F⁺ F⁺ in the plane perpendicular to P(B⁺)

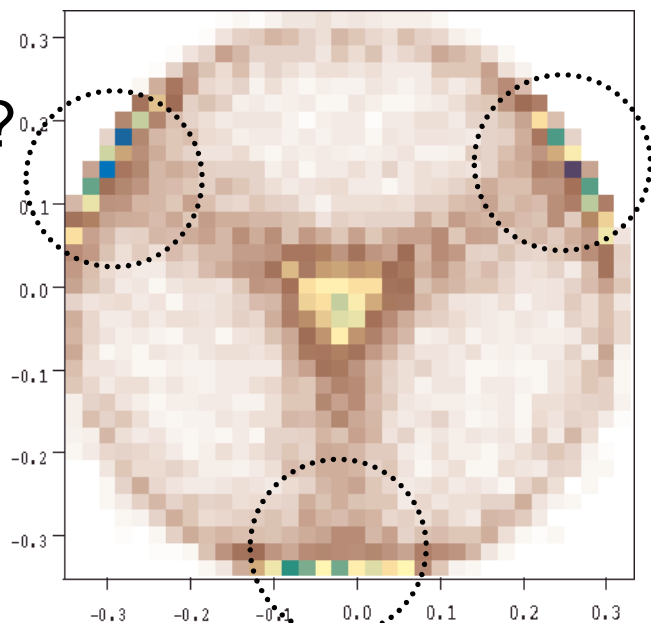
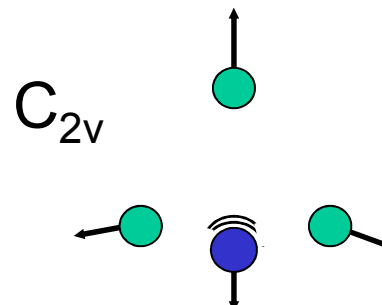
B1s ionization

F⁺ have similar
momenta \mathbf{P}^{\perp} \Rightarrow symmetric stretching

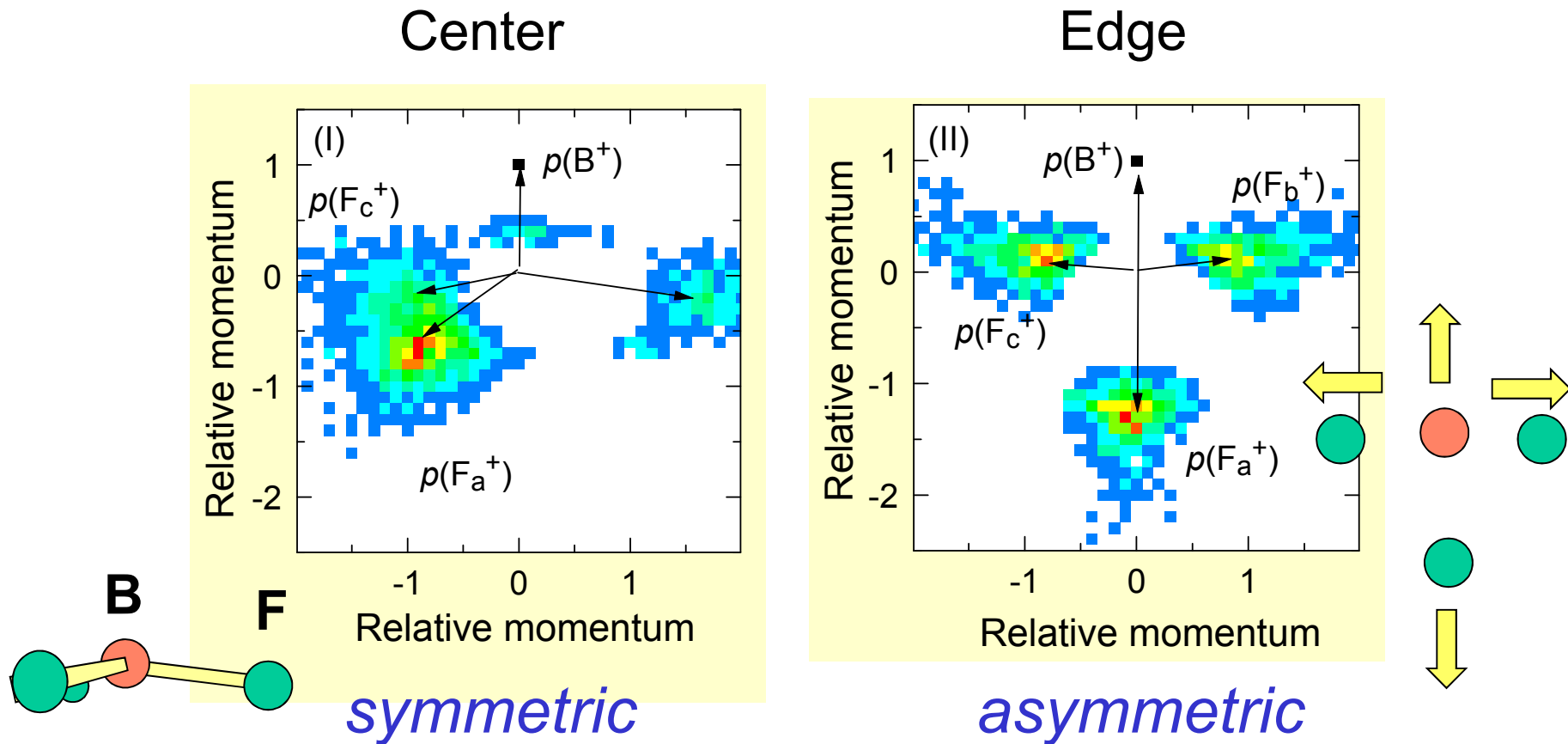


F1s ionization

asymmetric sharing of
momenta \mathbf{P}^{\perp}



Newton diagrams for symmetric and asymmetric nuclear motion probed by quadruple ion momentum imaging



Asymmetric nuclear motion as result of symmetry breaking by F 1s ionization has been detected for the first time via *quadruple ion momentum imaging*.

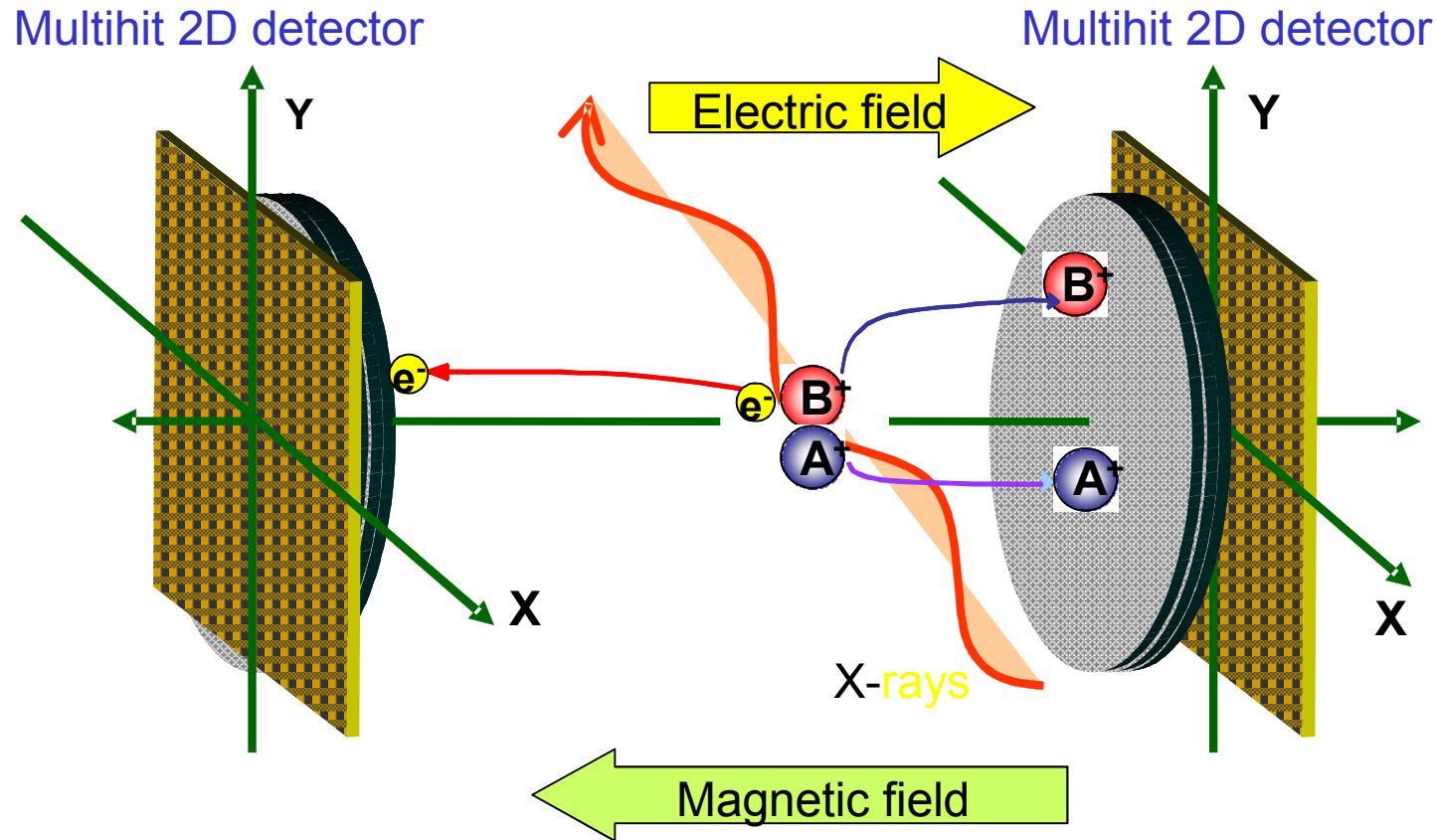


*Sendai
in summer*



Tanabata festival

Electron-ion coincidence momentum imaging



Ion-ion coincidence

→ Molecular axis

Ion momentum conservation

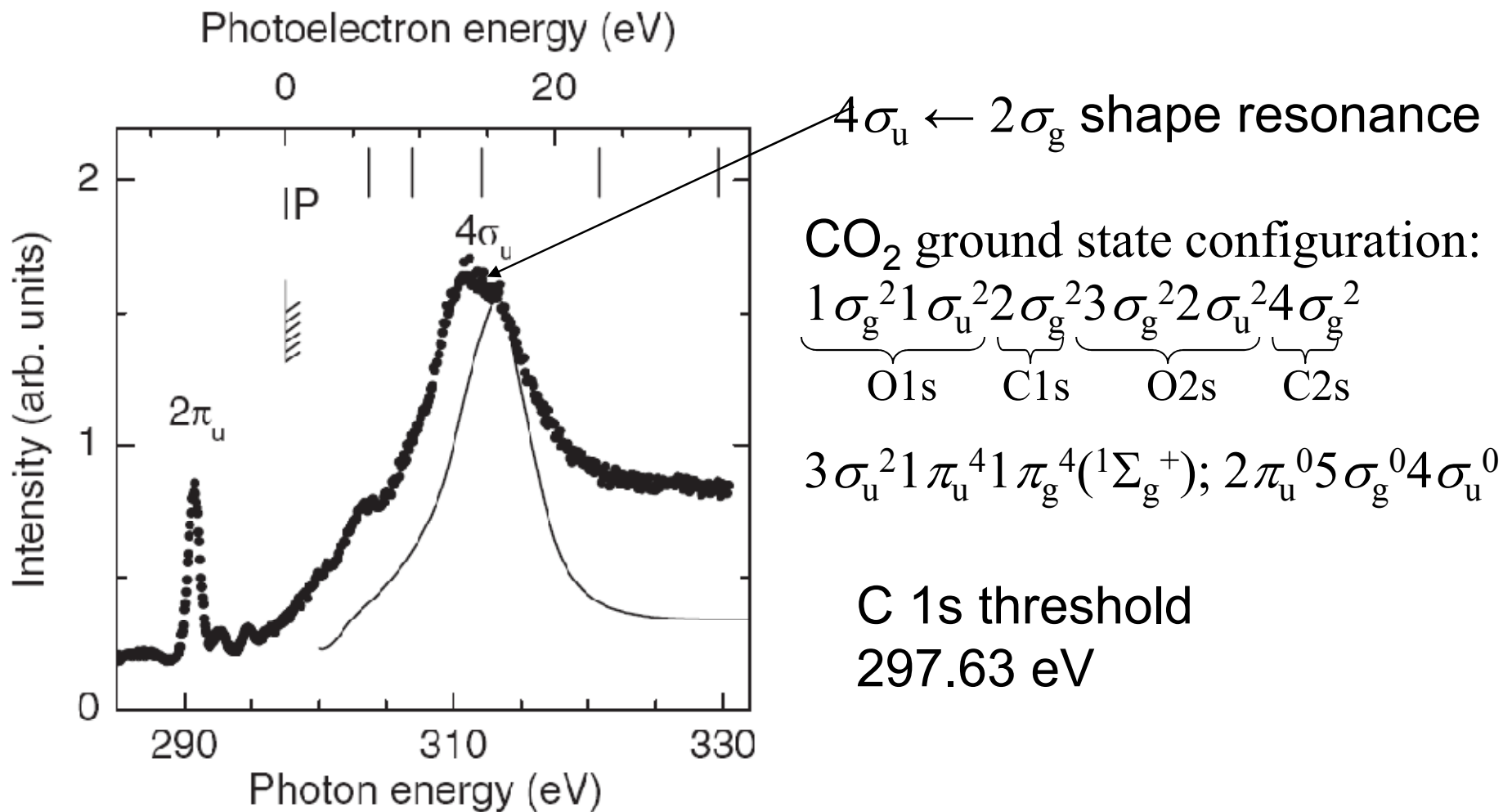
→ Retrieval of the source point

Electron-ion-ion coincidence

→ Molecular-frame e^- angular distribution

Towards photoelectron diffraction measurement

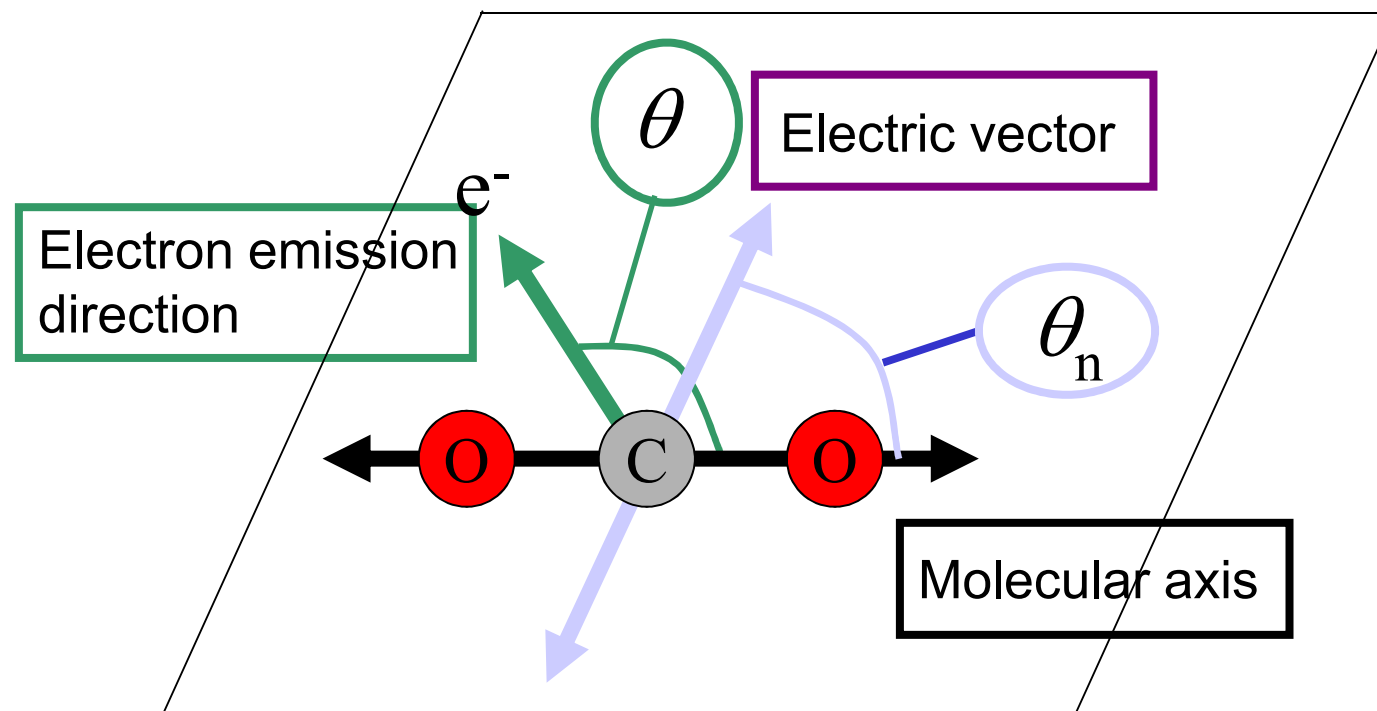
Total electron yield spectrum of CO_2 in the C1s ionization region



N. Saito *et al.*, J. Phys. B, **36** L25 (2003).

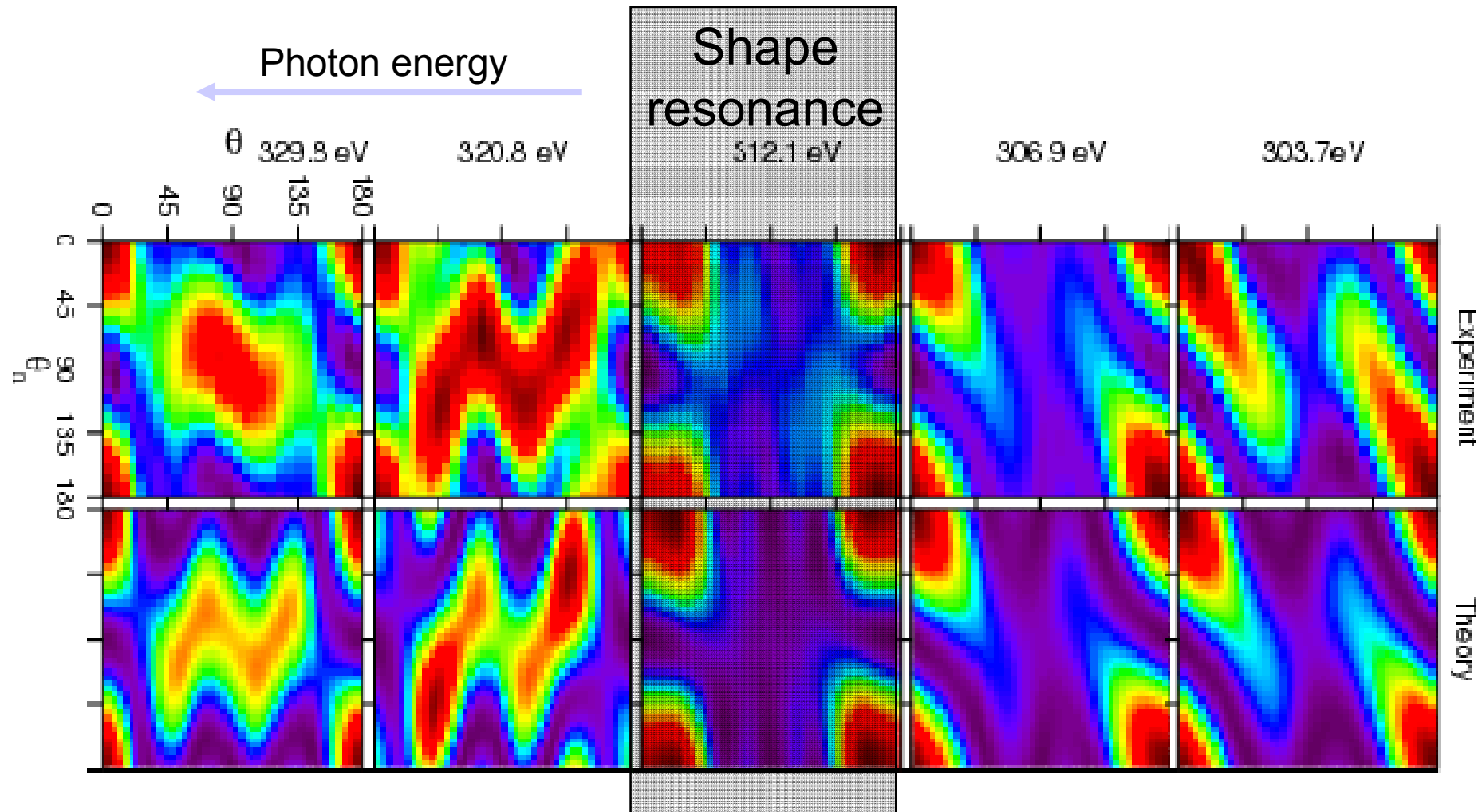
Reaction plane

Reaction plane = plane defined by the E vector and molecular axis



We focus on the electron emission within this reaction plane

MFPADs for C1s emission from CO₂: comparison between experiment and theory

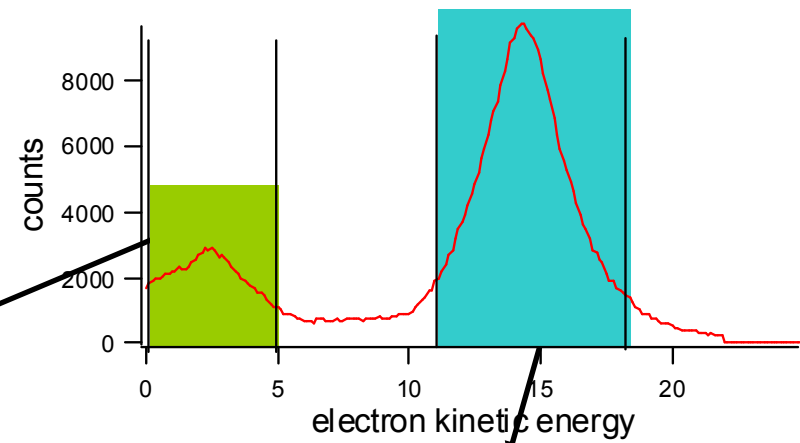
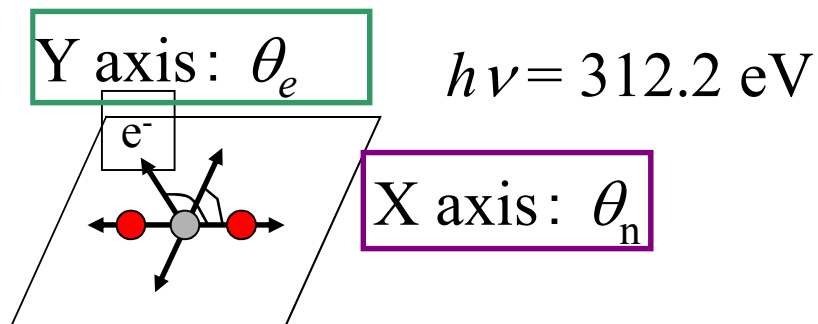


The general agreement between experiment and theory is reasonable.

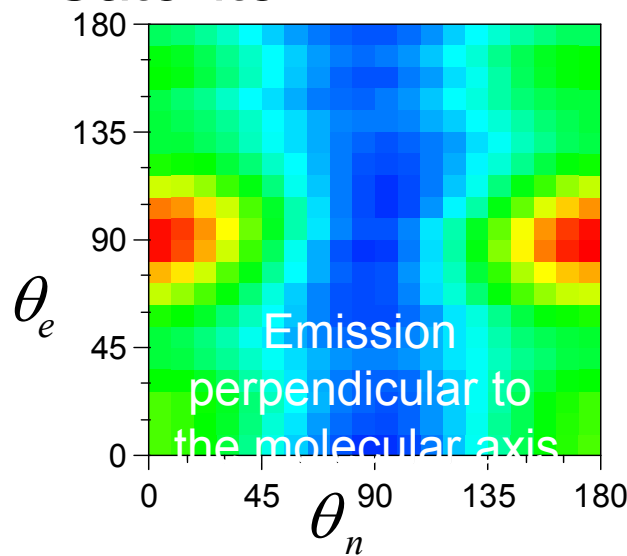
Liu *et al.* Phys. Rev. Lett. **101**, 083001(2008).

Satellite line vs Main line

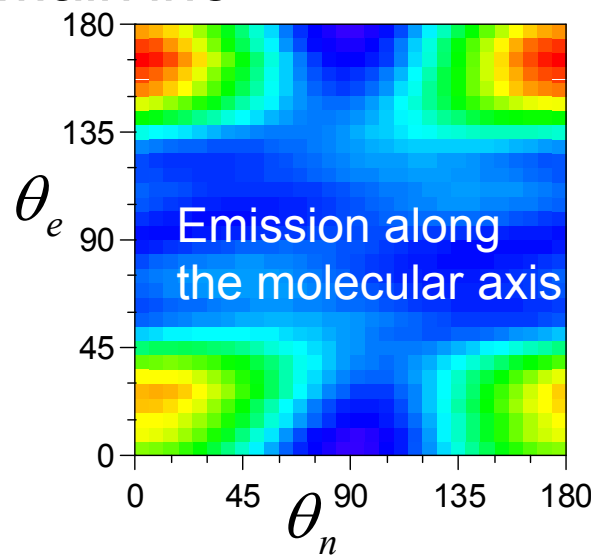
Photoelectron spectrum



Satellite



Mainline

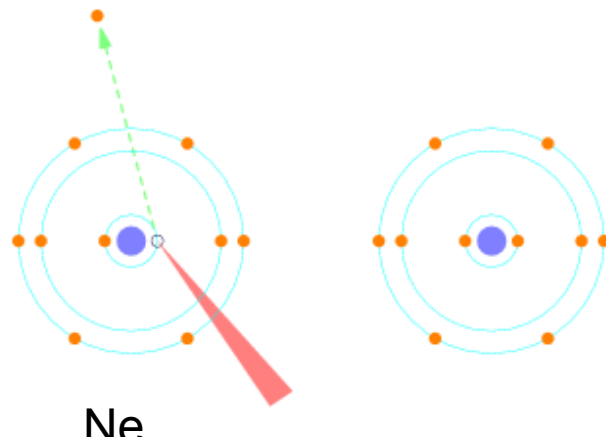


In both cases, the intensity drop at $\theta_n = 90^\circ$ i.e. $\Sigma - \Sigma$ parallel transition.
The electron emission directions are completely different.

Liu *et al.* Phys. Rev. Lett. **101**, 023001 (2008).

Auger vs Interatomic Coulombic Decay (ICD)

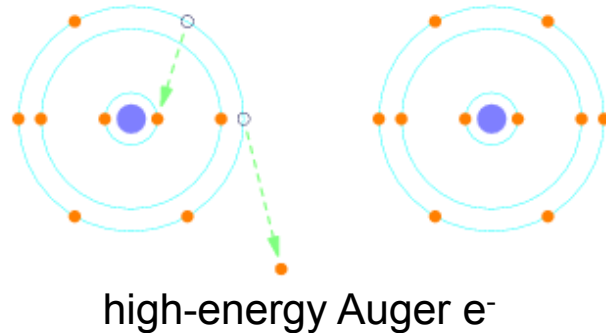
(a) Core ionization



Ne

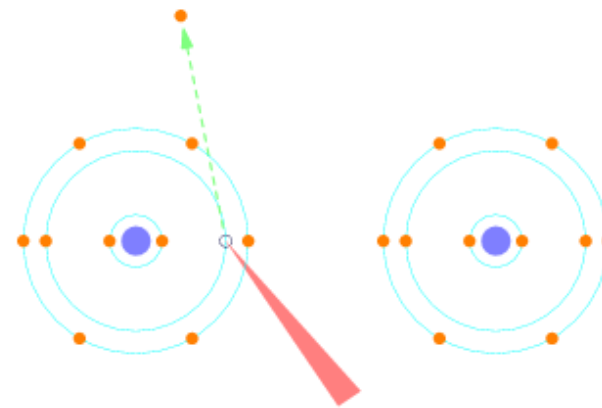
(b) Auger decay: One site state

Intra-atomic



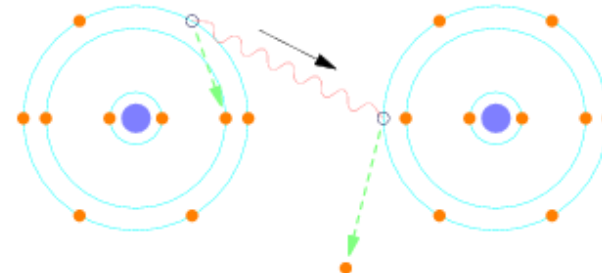
high-energy Auger e^-

(a) Inner-valence ionization



(b) ICD decay: two site state

Energy transfer via virtual photon exchange



low-energy ICD e^-

ICD rate is R dependent!

Interatomic Coulombic Decay (ICD)

Theoretical

First prediction - HF cluster:

L.S. Cederbaum, J. Zobeley, and F. Tarantelli, Phys. Rev. Lett. 79, 4778 (1997).

Prediction - Ne dimer:

R. Santra, J. Zobeley, L.S. Cederbaum *et al.*, Phys. Rev. Lett. 85, 4490 (2000).

Prediction - ICD from Auger final states in Ne dimer:

R. Santra and L.S. Cederbaum, Phys. Rev. Lett. 90, 153401 (2003).

Experimental

First observation - Ne cluster:

U. Hergenhahn and coworkers, Phys. Rev. Lett. 90, 203401 (2003).

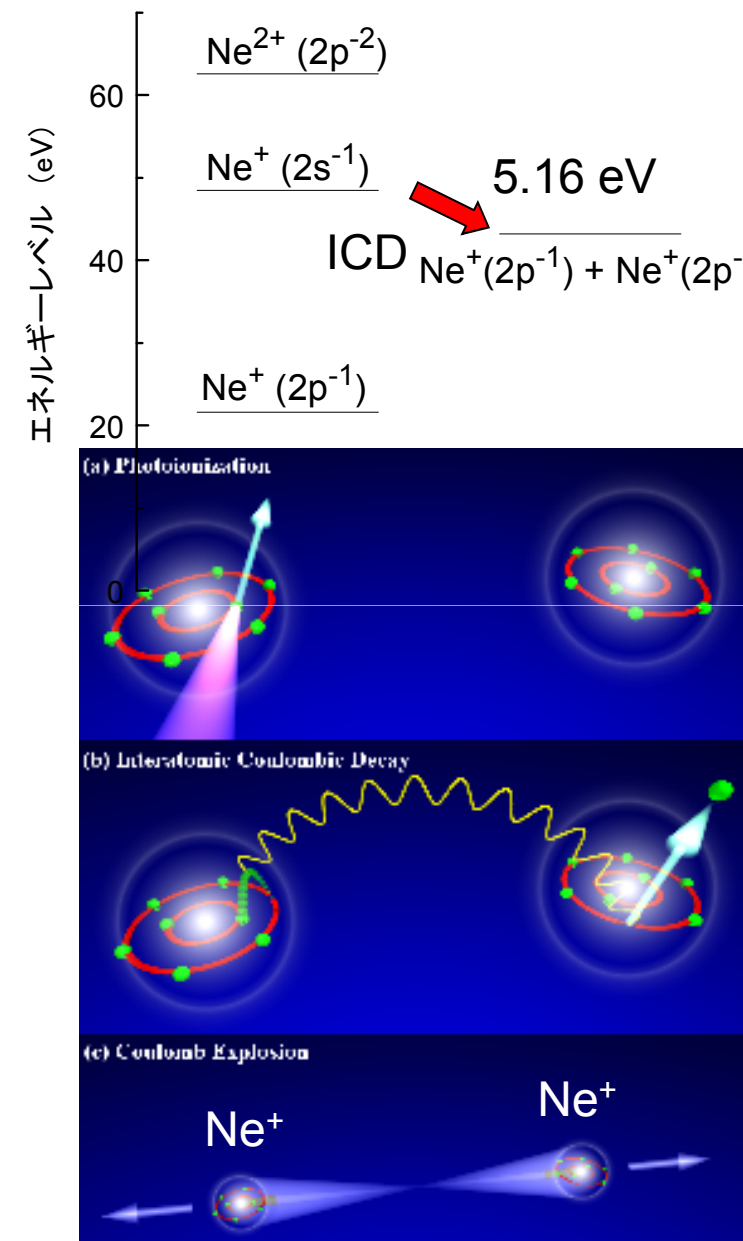
Cluster-size-dependent lifetime:

G. Öhrwall *et al.*, Phys. Rev. Lett. 93, 173401 (2004).

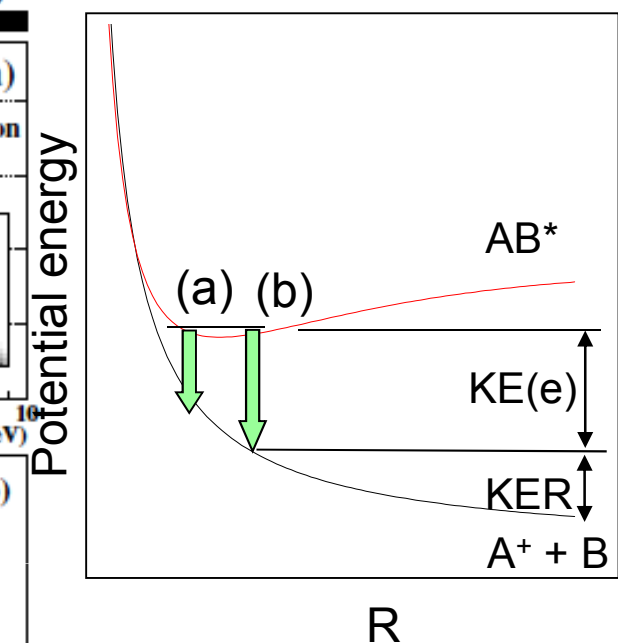
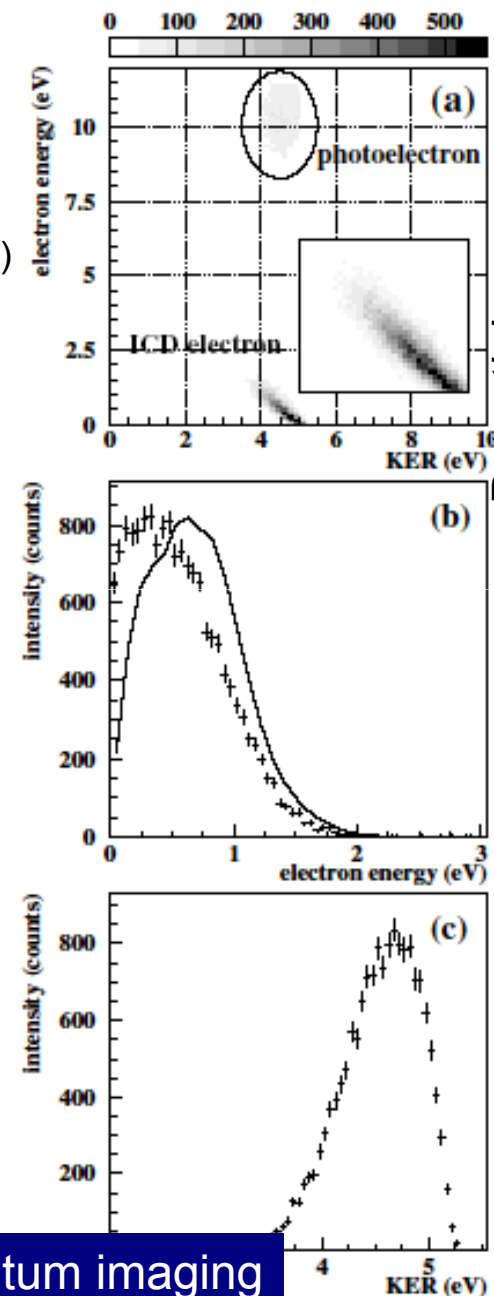
Ne₂ e-ion-ion coincidence:

R. Dörner and coworkers, Phys. Rev. Lett. 93, 163401 (2004).

Observation of ICD in Ne_2 by Frankfurt group

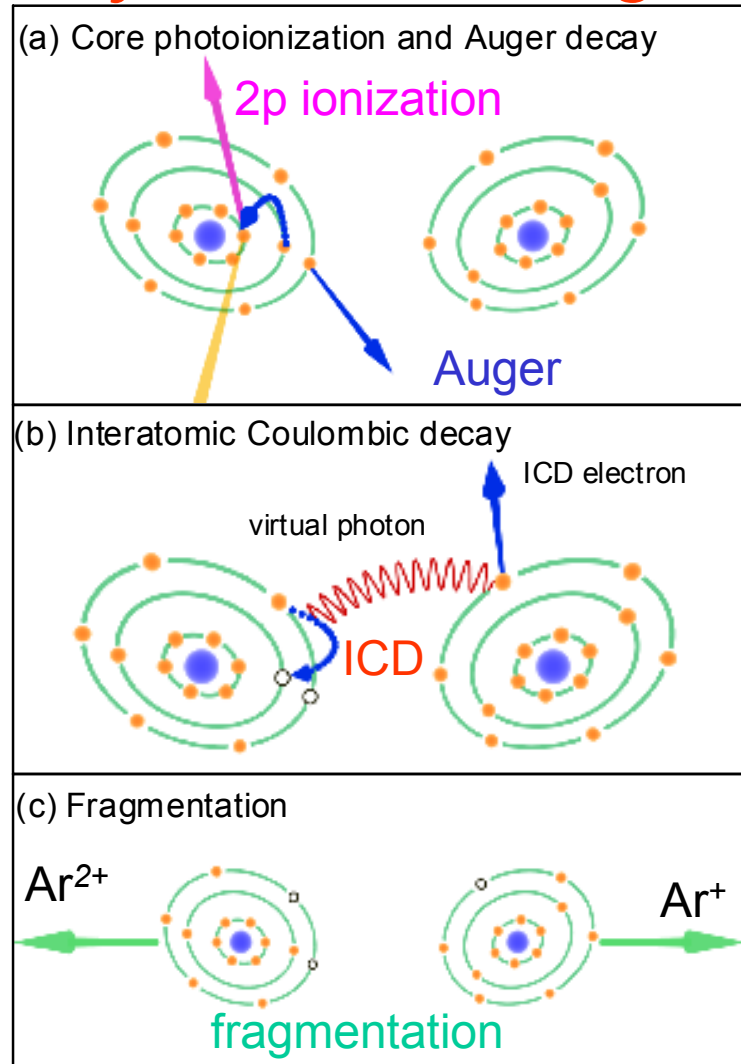


Electron-ion-ion coincidence momentum imaging



T. Jahnke *et al.*
Phys. Rev. Lett.
93, 163401 (2004)

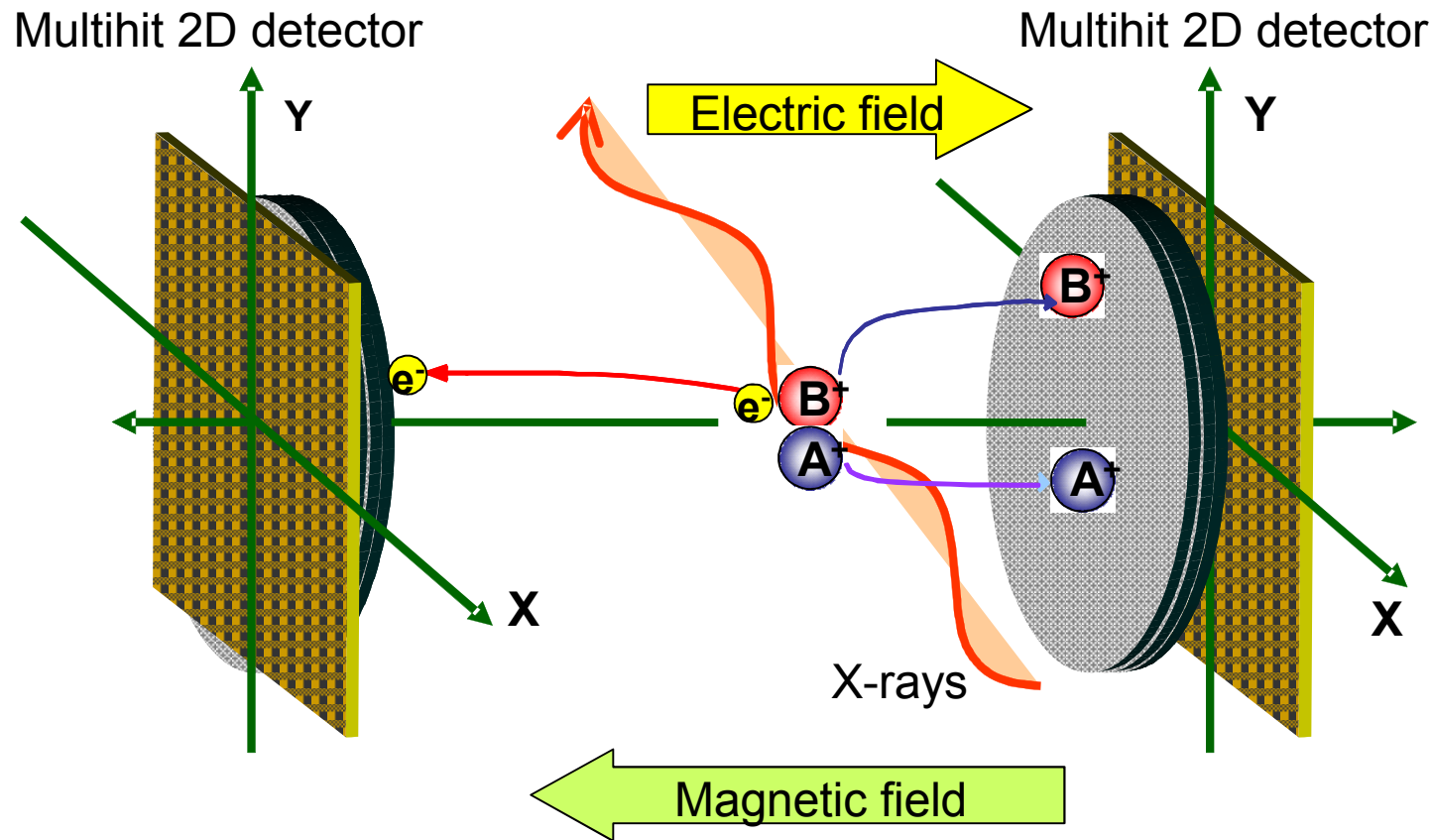
Experimental evidence of interatomic Coulombic decay from the Auger final states in argon dimers



Morishita *et al.* Phys. Rev. Lett. **96**, 243402 (2006).

We detect ICD electrons in coincidence with Ar^+ and Ar^{2+} using e-i-i coincidence momentum spectroscopy

Multiple coincidence momentum imaging



position & time of flight (x,y,t)



3D momentum of each particle

Multiple coincidence



Momentum correlation
among the particles

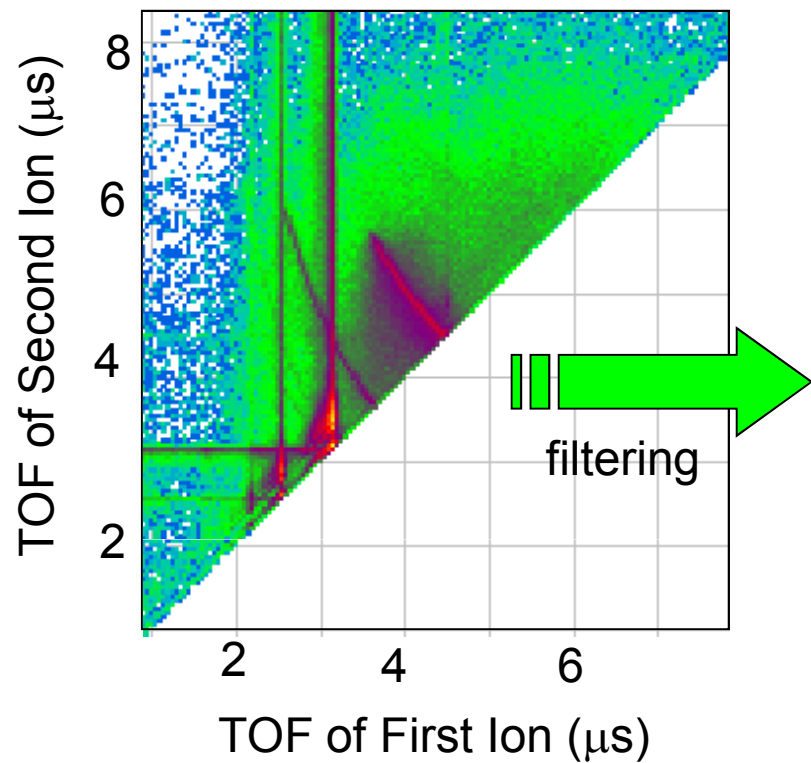
Momentum conservation



Selection of Dimer from others !

*Ar*₂

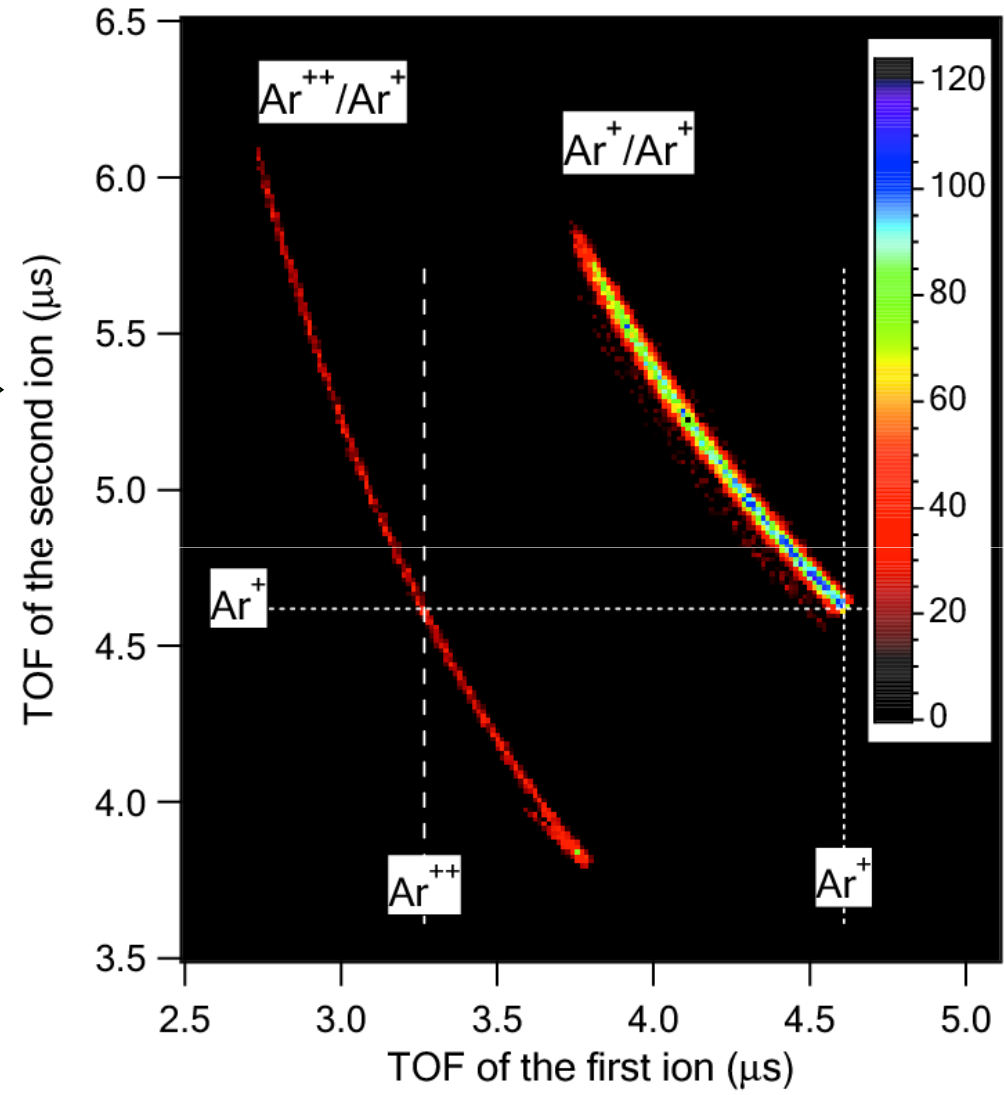
PIPICO spectrum



Filter conditions:

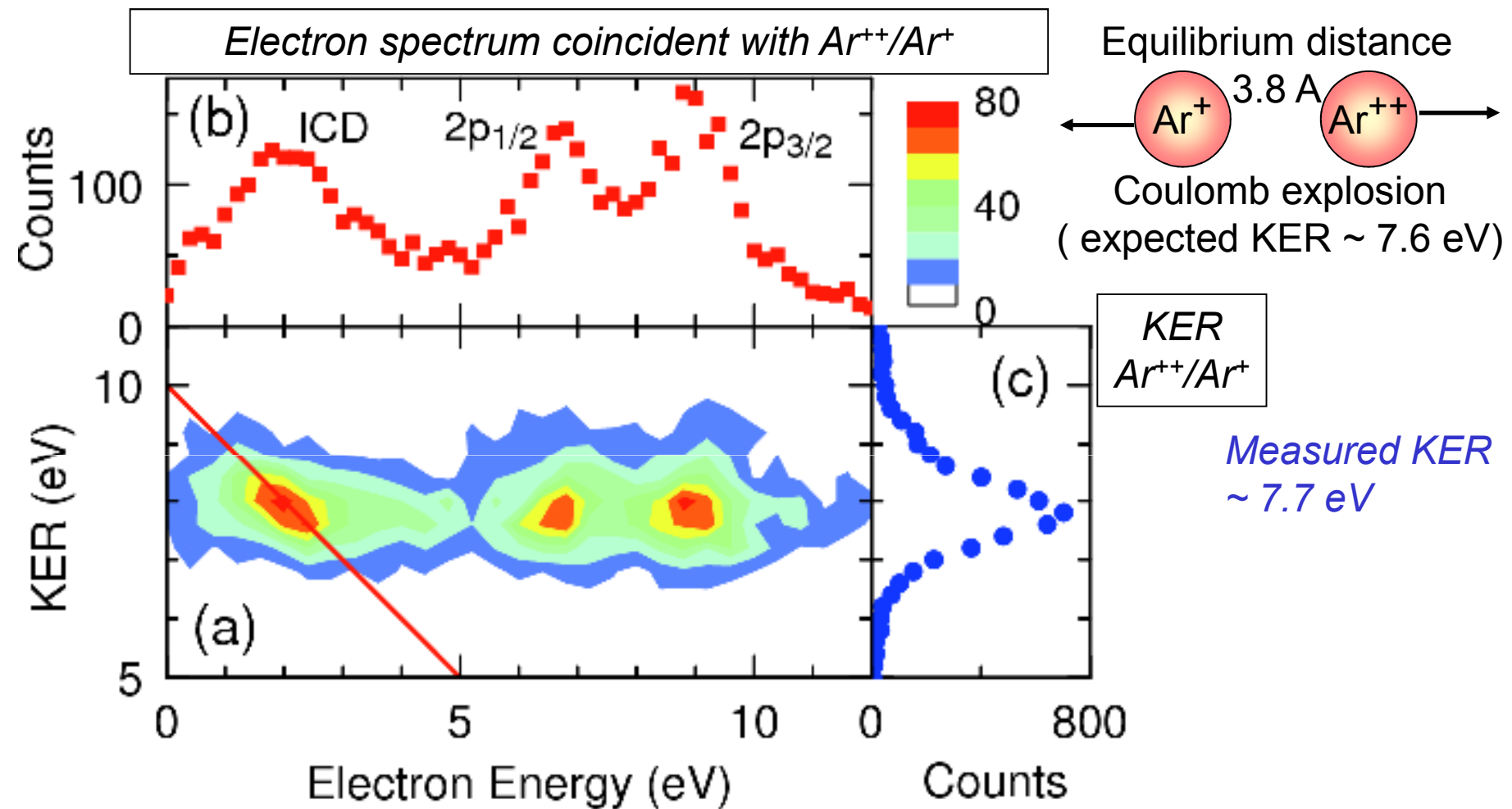
Ar^+/Ar^+ : the sum of the momentum of Ar^+ and $\text{Ar}^+ \sim 0$

$\text{Ar}^{++}/\text{Ar}^+$: the sum of the momentum of Ar^{++} and $\text{Ar}^+ \sim 0$



$\text{Ar}^{++}/\text{Ar}^+$ comes from ICD !?

Electron spectrum, KER, and their correlation



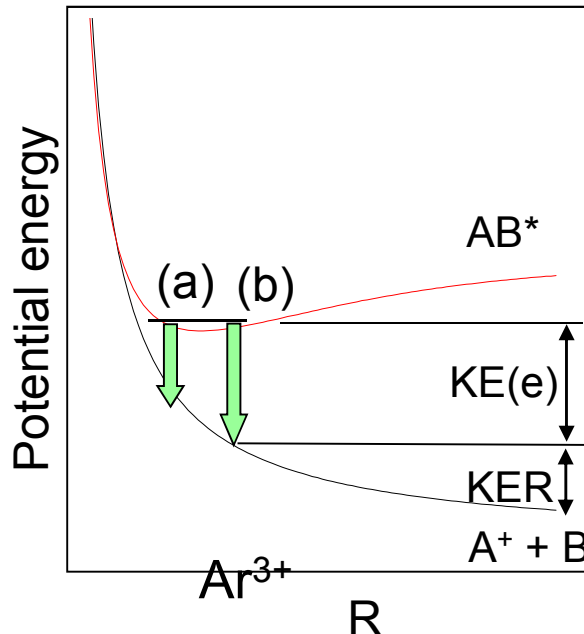
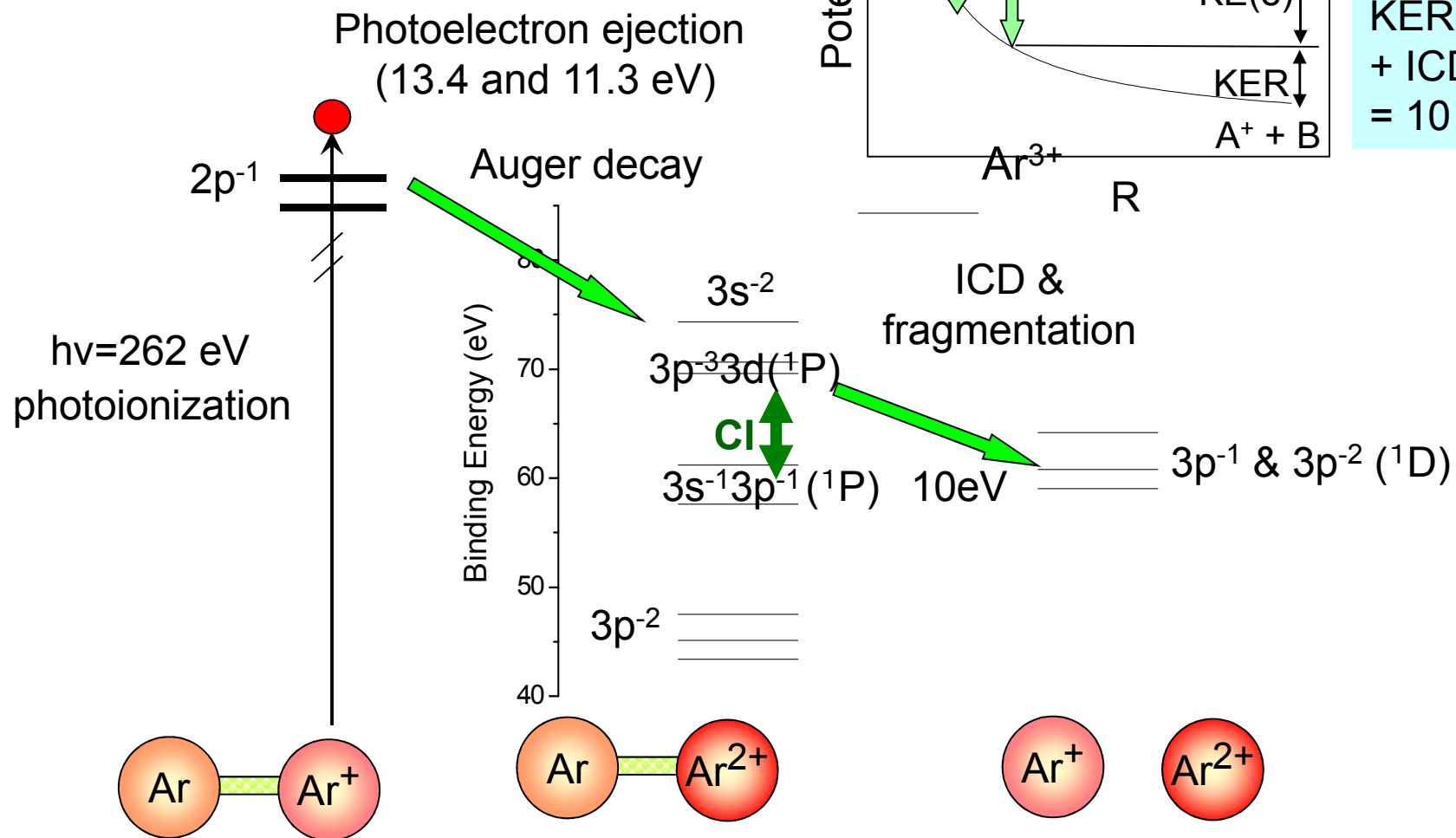
ICD: KER + KE(ICD electron) ~ constant

Islands of slope -1 are ICDs !

Breakup following ICD takes place almost instantaneously.

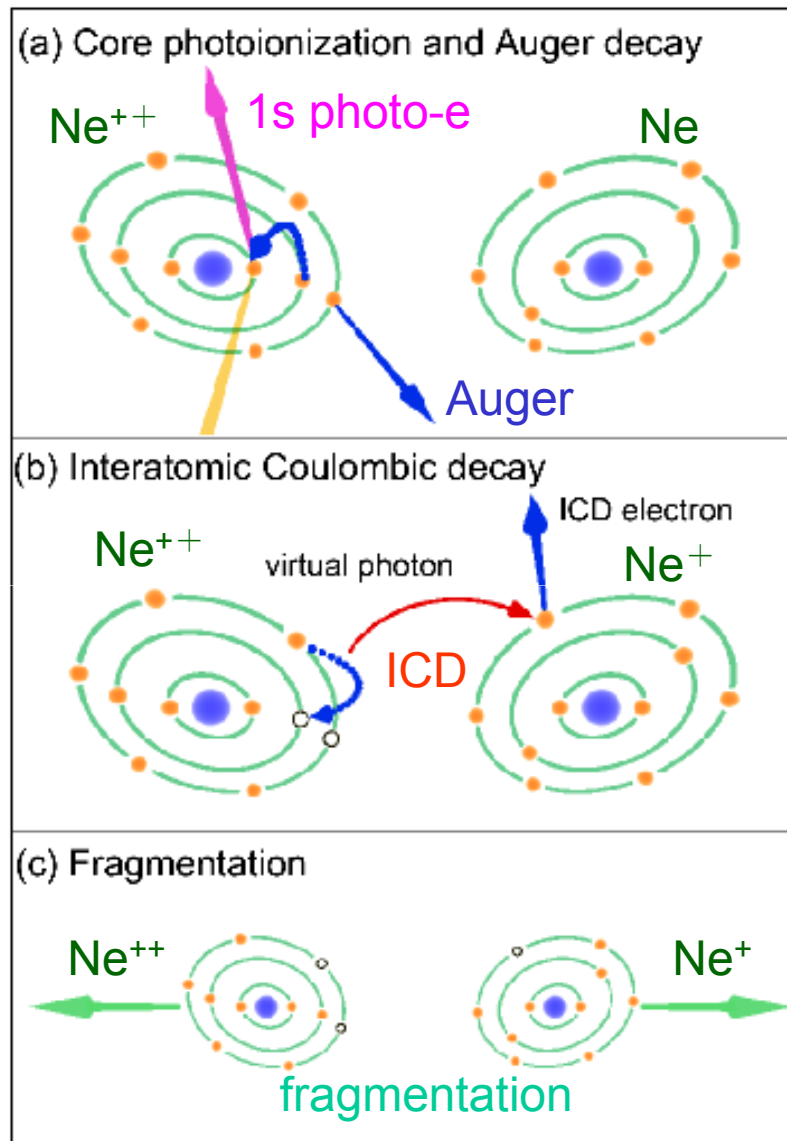
ICD is very fast!

Energy diagram of the ICD process in Ar₂



$$\begin{aligned} \text{KER} \\ + \text{ICD electron} \\ = 10 \text{ eV} \end{aligned}$$

ICD from the Auger final states in Ne dimer

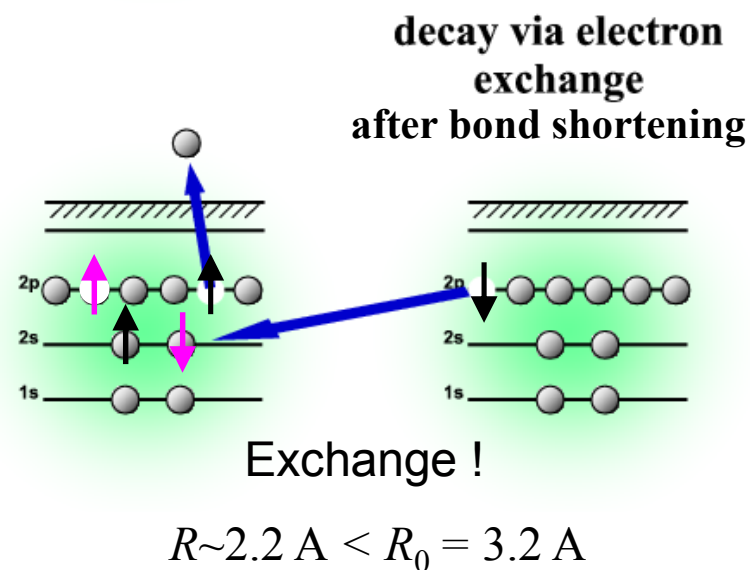
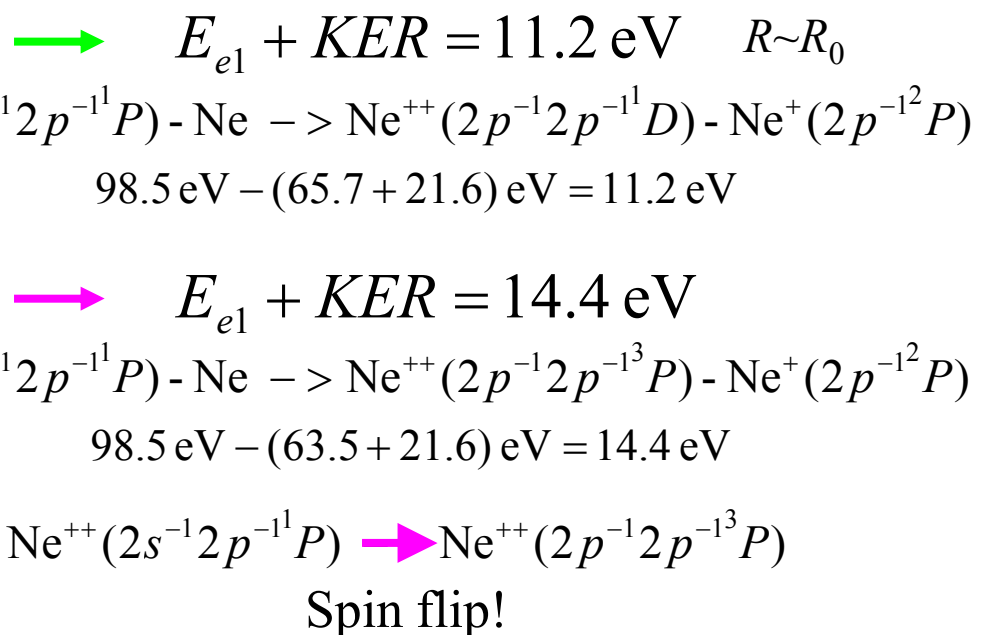
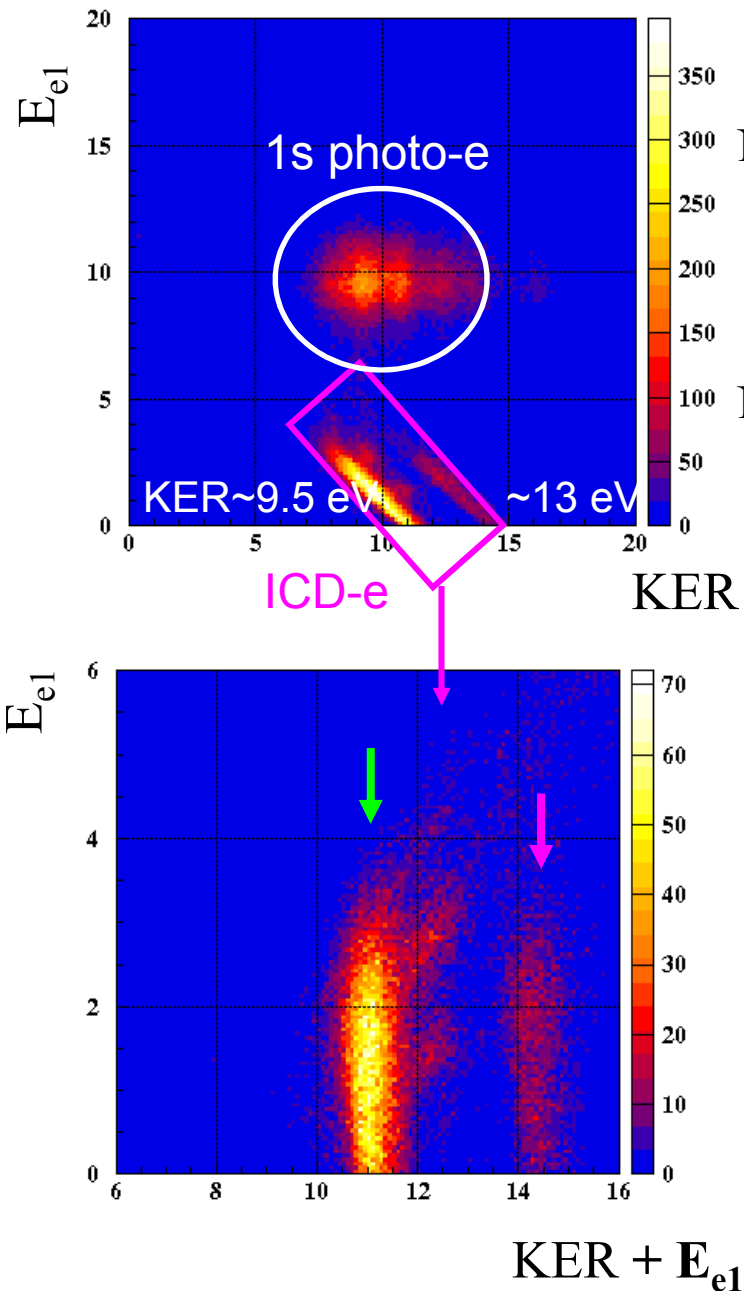


Kreidi et al. J. Phys. B. 41, 101002 (2008).



We detect ICD electrons in coincidence with Ne⁺ and Ne²⁺ using e-i-i coincidence momentum spectroscopy

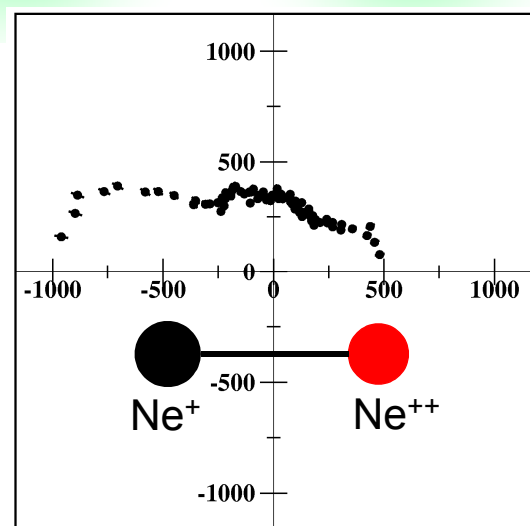
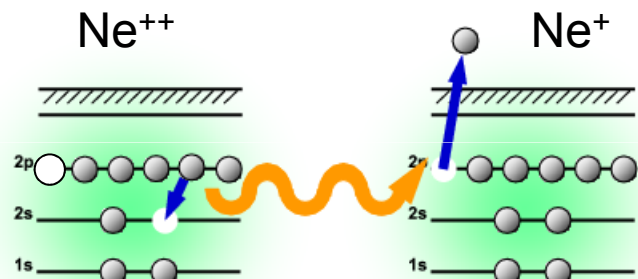
ICD channels in Ne_2 after KL_1L_{23} Auger



Molecular frame electron angular distributions emitted via ICD

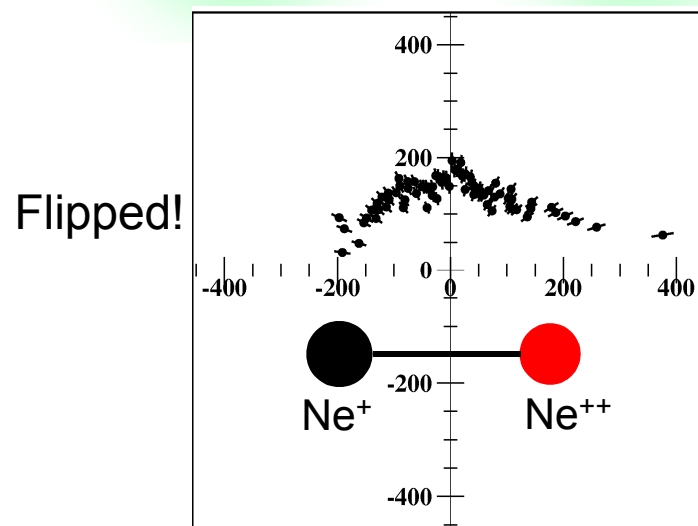
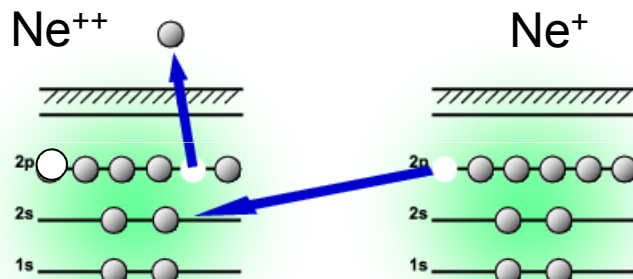
ICD by virtual photon exchange
(direct integral)
ICD electron is emitted from Ne^+ site

decay via virtual photon exchange

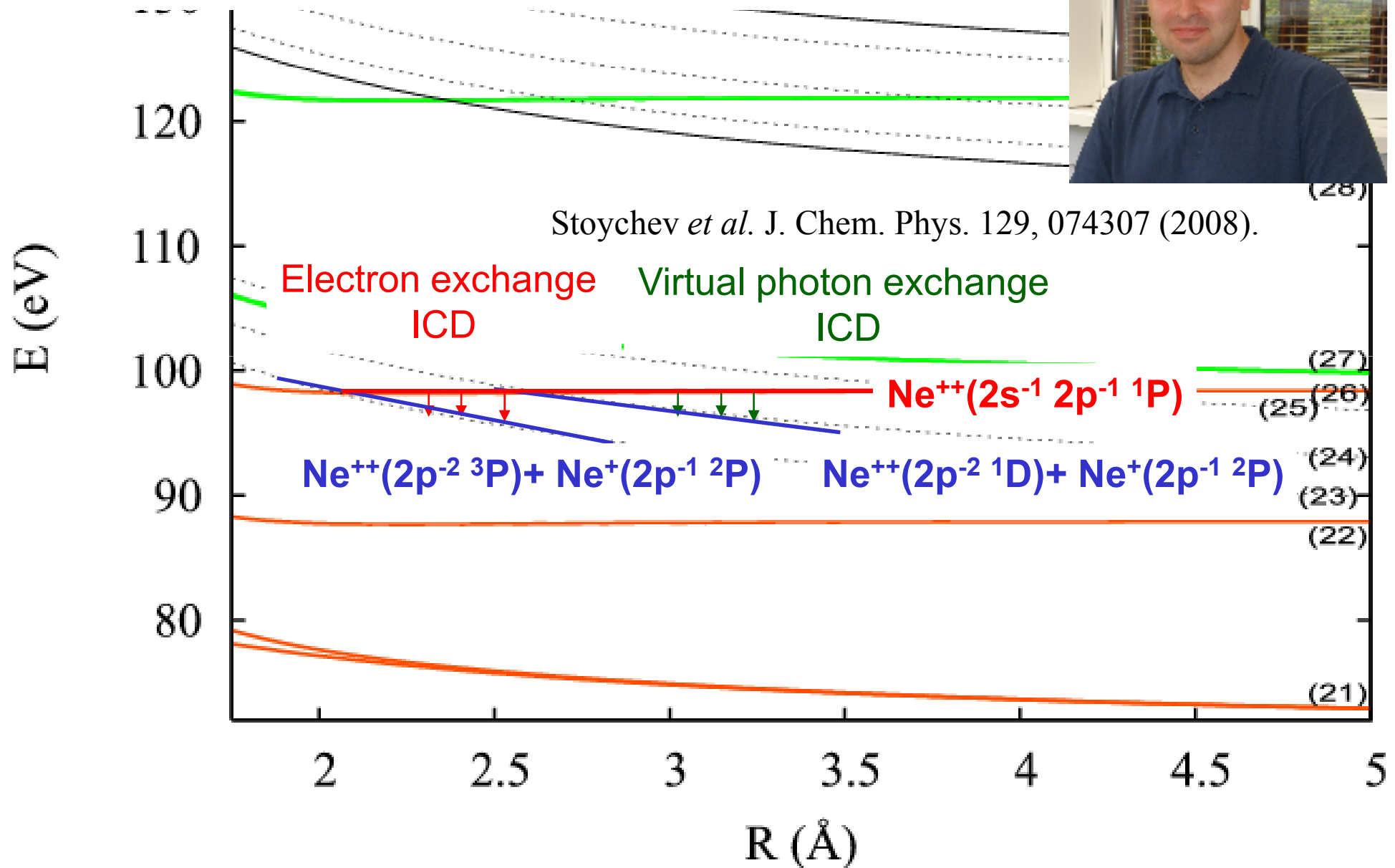
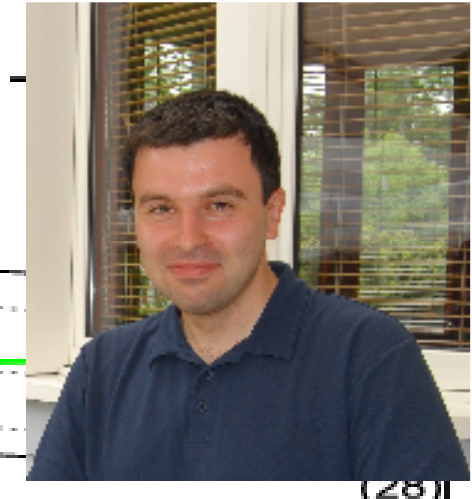


ICD by electron transfer
(exchange integral)
ICD electron is emitted from Ne^{++} site

decay via electron exchange



Wave packet dynamics on *ab initio* potential energy curves



The end

Thank you very much for your attention!

